We thank the reviewers for their comments. All comments are addressed below. Reviewers' comments are included in italics, our responses are included in cyan, and updated manuscript text is included in red.

Reviewer 1

The authors present a very valuable new dataset focusing on the organic fraction of submicron aerosol composition in Delhi, India from January 2017 to March 2018. Importantly, the dataset covers two winter seasons, which are the periods of most intense pollution in Delhi. To my knowledge this dataset is the first of its kind and provides significant insight into the nature and possible sources of PM2.5 in Delhi. I believe it should be published after a few minor points are addressed. In some places including the abstract the authors have referred to this study as a "source apportionment." While it is clear that this data and analysis have provided very important insight into possible sources/formation pathways for OA in Delhi, apportionment is a stronger term. I think the authors would agree that they have not identified the fraction of OA in Delhi originating from various specific anthropogenic and biogenic sources.

Response: We agree with the reviewer that the analysis does not conduct source apportionment with regards to the differences between anthropogenic and biogenic sources. However, our analysis allows us to separate organic aerosol (OA) of primary versus secondary origin, and to separate primary traffic-related OA from biomass burning OA in Spring 2018. The limited number of primary sources identified is likely due to the unit mass resolution of the ACSM, as has been observed previously (Aiken et al., 2009; Elser et al., 2016; Al-Naiema et al., 2018).

Therefore, we suggest continuing with the use of the term "source apportionment" but have clarified the terminology in section 3, where we have added the following text:

"Source apportionment conducted in this work was limited to separating primary and secondary OA in all seasons (and further, primary into BBOA and HOA in Spring 2018). Further separation of the factors may be possible with high-resolution data combined with application of factor constraints (Aiken et al., 2009; Elser et al., 2016; Al-Naiema et al., 2018) and source-specific measurements such as metals/metal ions for combustion or biomass burning emissions (Jaiprakash et al, 2017), or α-methylglyceric acid for biogenic secondary OA (Srivastava et al, 2019)."

- A lot of real estate in the paper is devoted to figures which illustrate the PMF analysis but do not convey take-home messages for the reader. Consider moving those to SI.

Response: Based on the reviewer's comment, we have edited the manuscript to emphasize key take-home messages of each figure. We also agree with the reviewer that "a lot of real estate in the paper is devoted to figures which illustrate the PMF analysis", which is the focus of this paper. We have moved Figs. 3 and 8 into the SI. The slopes and correlation coefficients shown in the figures have been inserted into the main text. The following are updated portions in the text (Section 3):

"It is therefore not surprising, as shown in Fig. S8a–c, that the behavior of POA and OOA in combined organic-inorganic PMF is very similar to that of organic-only POA and OOA respectively (POA: Slope~1.08, Intercept~1.6, R^2~0.96, OOA: Slope~0.88, Intercept~-0.4, R^2~0.88)."

The other figures are essential for supporting results presented in the paper. Figure 1 introduces the broad similarity of PMF factor analysis with that expected based on analysis conducted elsewhere (Ng et al., 2011; Zhang et al., 2011). Using time series patterns, Fig. 2 summarizes seasonal variations in primary and secondary PMF components using the large amount of data that was collected as a part of the campaign. Additionally, given that this is the first long-term PMF analysis published for organic MS in Delhi, we believe that developing an understanding of diurnal patterns of different aerosol types is very important. Accordingly, Figs. 4-7 elucidate diurnal patterns associated with PMF factors that reflect insights into possible sources and formation pathways that would otherwise be difficult to convey.

- The results clearly show elevated organic aerosol concentrations in winter. However, overall PM concentrations are also higher in winter. A figure (or figure panel) showing the seasonal variation in the OA fraction of PM mass would be very helpful.

Response: A figure detailing the fraction of species detected as "Org" or organics in the ACSM has already been published (Fig. 3, Gani et al (2019)).

We have updated the text to reference that figure:

"Over the campaign, organics accounted for 53% of the submicron mass, followed by inorganics (36%, of which sulfate, nitrate, ammonium, and chloride contributed 13%, 8%, 9%, and 6% respectively) and black carbon (BC) (10%) (Gani et al., 2019, Fig. 3)."

References:

Aiken, A. C., Salcedo, D., Cubison, M. J., Huffman, J. A., DeCarlo, P. F., Ulbrich, I. M., Docherty, K. S., Sueper, D., Kimmel, J. R., Worsnop, D. R., Trimborn, A., Northway, M., Stone, E. A., Schauer, J. J., Volkamer, R. M., Fortner, E., de Foy, B., Wang, J., Laskin, A., Shutthanandan, V., Zheng, J., Zhang, R., Gaffney, J., Marley, N. A., Paredes-Miranda, G., Arnott, W. P., Molina, L. T., Sosa, G., and Jimenez, J. L.: Mexico City aerosol analysis during MILAGRO using high resolution aerosol mass spectrometry at the urban supersite (T0) — Part 1: Fine particle composition and organic source apportionment, Atmospheric Chemistry and Physics, 9, 6633–6653, https://doi.org/10.5194/acp-9-6633-2009, 2009.

Al-Naiema, I. M., Hettiyadura, A. P. S., Wallace, H. W., Sanchez, N. P., Madler, C. J., Cevik, B. K., Bui, A. A. T., Kettler, J., Griffin, R. J., and Stone, E. A.: Source apportionment of fine particulate matter in Houston, Texas: insights to secondary organic aerosols, Atmospheric Chemistry and Physics, 18, 15 601–15 622, https://doi.org/10.5194/acp-18-15601-2018, 2018.

Elser, M., Huang, R.-J., Wolf, R., Slowik, J. G., Wang, Q., Canonaco, F., Li, G., Bozzetti, C., Daellenbach, K. R., Huang, Y., Zhang, R., Li, Z., Cao, J., Baltensperger, U., El-Haddad, I., and Prévôt, A. S. H.: New insights into PM2:5 chemical composition and sources in two major cities in China during extreme haze events using aerosol mass spectrometry, Atmospheric Chemistry and Physics, 16, 3207–3225, https://doi.org/10.5194/acp-16-3207-2016, 2016.

Gani, S., Bhandari, S., Seraj, S., Wang, D. S., Patel, K., Soni, P., Arub, Z., Habib, G., Hildebrandt Ruiz, L., and Apte, J. S.: Submicron aerosol composition in the world's most polluted megacity: the Delhi Aerosol Supersite study, Atmospheric Chemistry and Physics, 19, 6843–6859, https://doi.org/10.5194/acp-19-6843-2019, 2019.

Jaiprakash, Singhai, A., Habib, G., Raman, R. S., and Gupta, T.: Chemical characterization of PM1 aerosol in Delhi and source apportionment using positive matrix factorization, Environmental Science and Pollution Research, 24, 445–462, https://doi.org/10.1007/s11356-016-7708-8, 2017.

Ng, N. L., Canagaratna, M. R., Jimenez, J. L., Zhang, Q., Ulbrich, I. M., and Worsnop, D. R.: Real-time methods for estimating organic component mass concentrations from aerosol mass spectrometer data, Environmental Science & Technology, 45, 910–916, https://doi.org/10.1021/es102951k, 2011.

Srivastava, D., Favez, O., Petit, J.E., Zhang, Y., Sofowotee, U.M., Hopke, P.K., Bonnaire, N., Perraudin, E., Gros, V., Villenave, Albinet, A.: Speciation of organic fractions does matter for aerosol source apportionment. Part 3: Combining off-line and on-line measurements, Science of the Total Environment, 690, 944-955, https://doi.org/10.1016/j.scitotenv.2019.06.378, 2019.

Zhang, Q., Jimenez, J. L., Canagaratna, M. R., Ulbrich, I. M., Ng, N. L., Worsnop, D. R., and Sun, Y.: Understanding atmospheric organic aerosols via factor analysis of aerosol mass spectrometry: A review, Analytical and Bioanalytical Chemistry, 401, 3045–3067, https://doi.org/10.1007/s00216-011-5355-y, 2011.

Reviewer 2:

General comment The paper is focused on characterization of organic aerosol in New Delhi (India) using an ACSM and some additional measurements. The approaches used with PMF receptor model allow to get some information about the sources and the trends in primary and secondary organics. The topic is interesting, up-to-date and suitable for the Journal. In general, it is not easy to read this paper because most of the figures and results are reported in the supplementary material (73 pages) that seems to be richer than the main paper. Authors should think about bringing some of the main results in the paper removing them from the supplementary material. His at least for the results that authors say to be important like the relationships with PBL height or the influence of the ventilation coefficient. Further, there are some aspects that are not clear (see my specific comments) that should be addressed in a revision step.

Response: We recognize that there is a lot of material included as supplemental information. This is necessary for justification and interpretation of the 12 PMF factor analyses presented in this work. We did not include the information in the main manuscript for readability. .

Specific comments
Abstract. Thermodynamic modelling. What kind of modelling and for what?

Response: We conducted phase equilibrium modeling of aerosols using the extended aerosol inorganics model (E-AIM) to estimate the gas phase concentrations, and to obtain total concentrations after combining it with measured PM concentrations.

In the revised manuscript, we have updated the text (Abstract):

"Phase equilibrium modelling of aerosols using the extended aerosol inorganics model (E-AIM) predicts equilibrium gas-phase concentrations and allows evaluation of the importance of ventilation coefficient (VC) and temperature in controlling primary and secondary organic aerosol."

Abstract (and also in the main text). Authors speak of inter-annual variability, however, having only 15 months of measurements, the possibility to see an inter-annual trend is optimistic to say the least. I would suggest to change this aspect.

Response: We agree with the reviewer that 15 months of data provides limited information on interannual variability. There are very few campaigns in India taking systematic year-on-year measurements of particle concentrations and composition for entire seasons at 1 minute time resolution. This makes the collected dataset detailed enough to capture interannual variability between the winters and springs of 2017 and 2018.

We have rephrased "interannual variability" in the manuscript as "interannual variability between the winters and springs of 2017 and 2018".

Page 2 (line 8). Molecular markers such as...?

We have updated the text to be more specific (Section 1):

"They attribute chloride to sources such as coal combustion and biomass and waste burning using molecular markers. For example, hopanes such as S and R homohopane isomers are tracers for coal combustion, PAHs such as phenanthrene and benzo(a)anthracene are tracers for coal and biomass burning, and sugar anhydrosaccharides such as levoglucosan and mannosan are tracers for wood/biomass combustion (Pant et al., 2015). They also attribute higher winter concentrations to condensation of semivolatile ammonium nitrate and ammonium chloride during low-temperature conditions, weaker wind speeds, and shallow atmospheric boundary layer in the winter season (Pant et al., 2015, 2016a). In recent years, detailed source-specific profiles of combustion and non-combustion sources in the Southeast Asian region have been developed as a part of studies such as the Nepal Ambient Monitoring and Source Testing Experiment (NAMaSTE) campaign; for example, to discern between garbage burning and dung

burning, tracers such as 1,3,5-Trimethylbenzene and coprostanol respectively have been identified (IIT Bombay, 2008; Stockwell et al, 2016; Goetz et al., 2018; Jayarathne et al., 2018)."

Page 2 (lines 21-32). I agree that the high temporal resolution could furnish additional information compared to receptor models applied to 24h samples. However, in the case of using ACSM only some chemical species are available and there are limitations due to the missing information on metals and other compounds (for example levoglucosan and similar). This aspect should be clearly mentioned and a reference to the recent work of Belis et al (Atmospheric Environment 123 (2015) 240e250) regarding PMF and receptor models performances should be added.

Response: While non-refractory molecules are heavily fragmented by the electron impact ionization within the ACSM, some ion fragments have been identified as tracer ions for specific parent molecules, such as those at m/z 60 and 73 for levoglucosan (Ng et al., 2011). The limited importance of other species such as metals contributing to PM_1 in Delhi is suggested by the strong correlations (R^2 of 0.85 and slope of 0.96) of the ACSM based PM_1 + BC concentrations with SMPS-PM_1 estimates. Details of these correlations can be found in Gani et al (2019). Additionally, as Gani et al (2019) notes, "most of the PM1 was composed of non-refractory material and BC was consistent with past literature from Delhi which observed that metals and other non-refractory crustal materials, which we did not measure in this study, constituted less than 5% of PM_1 (Jaiprakash et al., 2017)."

As per the reviewer's suggestion, we have updated the text (Section 2.1):

"PMF2 has been identified as an appropriate receptor modeling technique that can be deployed for quantifying source contributions for air quality management (Belis et al., 2015)".

In addition, we have updated the text elsewhere as well (Section 3):

"Source apportionment conducted in this work was limited to separating primary and secondary OA in all seasons (and further, primary into BBOA and HOA in Spring 2018). Further separation of the factors may be possible with high-resolution data combined with application of factor constraints (Aiken et al., 2009; Elser et al., 2016; Al-Naiema et al., 2018) and source-specific measurements such as metals/metal ions for combustion or biomass burning emissions (Jaiprakash et al, 2017), or α-methylglyceric acid for biogenic secondary OA (Srivastava et al, 2019)."

In addition, the updated manuscript includes a review of recent source apportionment studies on $PM_{2.5}$ in Delhi conducted using different techniques/data and how our results compare to the general conclusions of those previous studies:

In the introduction:

"Most receptor modeling studies have principally relied on a small number of daily or multi-day filter-based samples collected over temporally restricted sampling periods, thereby limiting the possible application of factor analysis techniques such as positive matrix factorization (PMF) to

quantify source contributions for entire seasons at the site. Further, despite Delhi being a continental site, multiple studies attribute significant portions of finer fractions of PM to a sea-salt origin (Sharma et al., 2014; Sharma and Mandal, 2017). Recent studies have also developed bottom-up emissions inventories for the National Capital Territory (NCT) region encompassing the city of Delhi (Guttikunda et al, 2013), and conducted multi-season multiple-site $PM_{2.5}$ source apportionment using bottom-up approaches (IIT Kanpur, 2016; ARAI and TERI, 2018). In these bottom-up studies, as well as similar studies across South Asia, emissions sources such as transport, industry, dust, household solid fuel use, and biomass and waste burning are shown to contribute substantially to $PM_{2.5}$ (Conibear et al., 2018; GBD MAPS Working Group, 2018; Guo et al., 2018; Apte and Pant, 2019). Although these studies accounted for primary organic carbon and secondary inorganic species such as sulfate and nitrate, they often provide limited information regarding secondary organics."

In the conclusion:

"Because many bottom-up source apportionment efforts for Delhi are based on local (<50-100 km) scale inventories of primary emissions, they may neglect the important contributions of regionally transported primary and secondary aerosol from upwind regions. Here, we demonstrate the importance of secondary aerosol formed via atmospheric processing. Nevertheless, our results are in broad agreement with these inventories: 1) colder seasons are accompanied by higher concentrations and more diverse sources, including higher biomass burning emissions, 2) a significant aerosol mass fraction in Delhi is attributable to non-local sources, and 3) industries are a significant source of fine particulate matter (Guttikunda and Calori, 2013; IIT Kanpur, 2016; ARAI and TERI, 2018). However, the lack of consistent emission inventories limits the feasibility of action plans like GRAP, given that their implementation restricts economic activity (CEEW, 2019)."

Section 2 (methods). ACSM is working on PM1 instead, other measurements have been done on PM2.5. Why not on the same size fraction? The differences should be explained. In addition, BC, and UVPM are not shown at all in the main paper but only in the supplementary material is this meaning that these species are not so important in the framework of the results?

Response: The ACSM and AE33 deployed for the Delhi Aerosol Supersite (DAS) study are suitable for measuring PM_1 and $PM_{2.5}$ respectively. However, both instruments were on sampling lines with $PM_{2.5}$ cyclones (50% cutoff for aerosols 2.5 μm in diameter). Also, the sum of hourly averaged PM_1 concentration (measured by the ACSM) and BC concentrations (measured by the AE33) at this site are correlated to $PM_{2.5}$ measured at the nearest monitoring station operated by the Delhi Pollution Control Committee (DPCC), R.K. Puram (3 km away) with a slope of ~0.85, R^2~0.6 (Gani et al., 2019). This suggests that a PM_1 inlet likely captures the bulk of $PM_{2.5}$ aerosols.

At the time, the PM_1 inlet was standard for online aerosol mass spectrometers. Measurement of $PM_{2.5}$ requires the use of a different aerodynamic lens and vaporizer. Laboratory evaluation of the $PM_{2.5}$ system, published a few months prior to the beginning of our campaign, showed that the new vaporizer produced markedly different ion fragmentation patterns of aerosols (Xu et al., 2016). The consistency of fragmentation patterns is essential for factor identification using

reference profiles from mass spectra obtained across the world (Ng et al., 2011). Therefore, we used the standard PM_1 inlet with the ACSM.

As for BC and UVPM, we use BC as a primary aerosol tracer, with the Sandradewi model-based biomass burning component of black carbon (BC_{BB}) being used as one of the tracers for biomass burning. In addition, we use ΔC, the difference between UVPM and BC, as a tracer for biomass burning. Therefore, neither BC nor UVPM were included in the PMF analysis directly. Details of the tracer selection can be found in Section 2.2 Factor Selection.

Page 3 (section 2.1). Fifteen months divided into six seasons, why not using calendar seasons, I mean one year divided in four seasons?

Response: Delhi's climate is not clearly defined by the four seasons that are commonly used in many other countries, as there are five distinct periods. In this work and Gani et al (2019), we have used the Indian National Science Academy's definition that classifies seasons based on temperature and climate. In effect, this definition divides one year into 5 seasons-winter, spring, summer, monsoon, and autumn.

Reference: Indian National Science Academy: Seasons of Delhi, https://www.insaindia.res.in/climate.php, 2018.

Section 2.2. How it is used CO? In the PMF? Again, no trace of CO is reported in the main text.

Response: In this study, carbon monoxide (CO) was not measured. Instead, when available, we used CO measured about 11 km (~7 miles) from our site at a fixed monitoring location RK Puram maintained by the Central Pollution Control Board (CPCB), Government of India, as an external traffic and combustion tracer.

We have updated the text (Section 2.2):

"In this study, carbon monoxide (CO) was not measured. When available, we used CO measured about 11 km (~7 miles) from our site at a fixed monitoring location RK Puram maintained by the Central Pollution Control Board (CPCB), Government of India, as an external traffic and combustion tracer."

Page 5 (lines 26-28). It is reported that OOA correlates strongly with both sulphate and nitrate. However, in several sites nitrate and sulphate have different seasonal trends with sulphate larger in the warm seasons and nitrate larger in the cold seasons because of its thermal instability. This is true for both ammonium nitrate and sodium nitrate coming from aged marine salt. If I have well understood there is a correlation between SOA with both nitrate and sulphate suggesting that at this they have the same trend. Is this true? In case it will be useful to discuss this aspect mentioning explicitly the similarity in these trends that is not often observed at other sites.

Response: In this study, we have conducted receptor modeling analysis using Positive Matrix Factorization (PMF) applied on organic mass spectra only and combined organic and inorganic mass spectra. While the OOA factor in PMF analysis conducted using organic mass spectra only

correlates with both nitrate and sulfate, in the combined organic and inorganic mass spectra based PMF analysis, OOA associated with nitrate and sulfate can be separated into OOA mixed with Ammonium Nitrate (AN-OOA) and OOA mixed with Ammonium Sulfate (AS-OOA) and the two components have different diurnal trends (Section 3.2.2, Fig. 6). Thus, the correlation of nitrate and sulfate with OOA in organic-only PMF analysis is likely a limitation of the technique when applied to the Delhi organic only MS dataset. As we have shown, this limitation can be addressed by explicitly including inorganic MS contributions in PMF analysis. This aspect has been discussed in detail in Sect. 3.2.2 and summarized in Sect. 4 Conclusions.

Page 5 (line 30-31). Actually, looking at Figure 2 POA and OOA seems quite comparable. Are the difference mentioned statistically significant?

Response: Since POA and OOA presented in Figure 2 are non-normally distributed (Gani et al., 2019) as is common for many environmental datasets, we conducted the two-tailed Kruskal-Wallis test and the Wilcoxon Signed Rank test. Results from both tests indicate that the overall distributions are significantly different ($p < 0.05$). For detailed differences of summary statistics between POA and OOA, we refer the reviewer to Table 3.

Page 7 (lines 9-10). This sentence is not correct because at night there is not a decreasing PBL, rather at sunset a new shallow boundary-layer is established generally thermally stable that could trap pollutants and will evolve at sunrise the day after mixing air from ground level with air masses above, see for example MeteorologischeZeitschrift, Vol. 21, No. 4, 385-398 (August 2012). I believe that authors should explain better this part.

Response:

We have updated the text (Section 3.1):

"We observed larger nighttime (1800–2200 hours) and smaller daytime (0600–0900 hours) POA peaks. As the sun sets, radiative cooling of the ground surface flips the ambient temperature profile in the surface layer, with ambient temperature increasing with altitude. This inversion layer is thermally stable and traps pollutants at nighttime. As the sun rises, radiative heating warms up the ground surface and the ambient temperature profile returns to a decreasing trend with altitude, which is thermally unstable. Thus, the nighttime and daytime periods encounter similar thermal transition phases, albeit in opposite directions (Figs. 3, S15) (Seinfeld and Pandis, 2016). However, the nighttime period is accompanied by minimal photochemical conversion of POA to SOA in the evening, confirmed by the lower OOA, AN-OOA, and AS-OOA concentrations in the evening (Sect. 3.2). These dynamics could explain the larger nighttime and the smaller daytime POA peaks."

Page 12 (lines 14-15). These percentages are really so different statistically?

Response: We conducted the Kruskal-Wallis test based one-tailed non-parametric multiple comparison tests for the 6 seasonal fractional contributions of POA. Indeed, overall distribution

of spring 2018 is significantly higher compared to the fractions in other seasons (p<0.05). However, spring 2017, winter 2017 and winter 2018 are statistically similar distributions.

We have updated the text (Section 3.3):

"The spring 2018 POA fraction varies between 34–75%, higher than the winters of 2017 and 2018 and spring 2017 (20–68%), and summer 2017 and monsoon 2017 (23–53%)".

Page 12 (lines 18-19). The larger primary emissions during cold months is not reflected in the percentages above because the maximum appears to be during spring.

Response: As shown in the previous response by the Kruskal-Wallis test, fractional contributions of POA in Spring 2017, with two factors only, are in line with the two winters. Spring 2018, on the other hand, is different from Spring 2017 due to the separation of an additional BBOA factor in that season. This separation likely resulted in the higher POA fraction in Spring 2018. Additionally, the Kruskal-Wallis test based one-tailed non-parametric multiple comparison tests show that temperatures in summer and monsoon are significantly higher than temperatures in springs which are significantly higher than those in the winters (p<0.05). Therefore, spring and winter can be generally categorized as the colder months whereas summer and monsoon as the warmer. Thus, using the term "colder" months is reasonable.

Figures 3b and 3c. The intercepts are missing, are they negligible?

Response: The intercept in figure 3b is 0.001 and in figure 3c is 7e-04, negligible in comparison to the fractional contributions being represented in the figures.

Figures 4, 5, 6, and 7. Please report in the caption what is the difference between continuous lines and marks.

Response: The captions specify that lines correspond to means and marks correspond to medians in the figures.

References:

Aiken, A. C., Salcedo, D., Cubison, M. J., Huffman, J. A., DeCarlo, P. F., Ulbrich, I. M., Docherty, K. S., Sueper, D., Kimmel, J. R., Worsnop, D. R., Trimborn, A., Northway, M., Stone, E. A., Schauer, J. J., Volkamer, R. M., Fortner, E., de Foy, B., Wang, J., Laskin, A., Shutthanandan, V., Zheng, J., Zhang, R., Gaffney, J., Marley, N. A., Paredes-Miranda, G., Arnott, W. P., Molina, L. T., Sosa, G., and Jimenez, J. L.: Mexico City aerosol analysis during MILAGRO using high resolution aerosol mass spectrometry at the urban supersite (T0) — Part 1: Fine particle composition and organic source apportionment, Atmospheric Chemistry and Physics, 9, 6633–6653, https://doi.org/10.5194/acp-9-6633-2009, 2009.

Al-Naiema, I. M., Hettiyadura, A. P. S., Wallace, H. W., Sanchez, N. P., Madler, C. J., Cevik, B. K., Bui, A. A. T., Kettler, J., Griffin, R. J., and Stone, E. A.: Source apportionment of fine particulate matter in Houston, Texas: insights to secondary organic aerosols,

Atmospheric Chemistry and Physics, 18, 15 601–15 622, https://doi.org/10.5194/acp-18-15601-2018, 2018.

Apte, J. S. and Pant, P.: Toward cleaner air for a billion Indians, PNAS, 116 (22), 10 614–10 616, https://doi.org/10.1073/pnas.1905458116, 2019.

ARAI and TERI: Source apportionment of PM2.5 and PM10 of Delhi NCR for identification of major sources. Available at http://www.teriin.org/sites/default/files/2018-08/Report_SA_AQM-Delhi-NCR_0.pdf, 2018.

Belis, C.A., Karagulian, F., Amato, F., Almeida, M., Artaxo, P., Beddows, D.C.S., Bernardoni, V., Bove, M.C., Carbone, S., Cesari, D. and Contini, D., 2015. A new methodology to assess the performance and uncertainty of source apportionment models II: The results of two European intercomparison exercises. Atmospheric Environment, 123, 240-250, https://doi.org/10.1016/j.atmosenv.2015.10.068, 2015.

CEEW: What is Polluting Delhi's Air? Understanding Uncertainties in Emissions Inventory. New Delhi: Council on Energy, Environment and Water, https://www.ceew.in/publications/what-polluting-delhi%E2%80%99s-air, 2019.

Conibear, L., Butt, E., Knote, C., Arnold, S. R., and Spracklen, D. V.: Residential energy use emissions dominate health impacts from exposure to ambient particulate matter in India, Nature Communications, 9, https://doi.org/10.1038/s41467-018-02986-7, 2018.

Elser, M., Huang, R.-J., Wolf, R., Slowik, J. G., Wang, Q., Canonaco, F., Li, G., Bozzetti, C., Daellenbach, K. R., Huang, Y., Zhang, R., Li, Z., Cao, J., Baltensperger, U., El-Haddad, I., and Prévôt, A. S. H.: New insights into PM$_{2.5}$ chemical composition and sources in two major cities in China during extreme haze events using aerosol mass spectrometry, Atmospheric Chemistry and Physics, 16, 3207–3225, https://doi.org/10.5194/acp-16-3207-2016, 2016.

Gani, S., Bhandari, S., Seraj, S., Wang, D. S., Patel, K., Soni, P., Arub, Z., Habib, G., Hildebrandt Ruiz, L., and Apte, J. S.: Submicron aerosol composition in the world's most polluted megacity: the Delhi Aerosol Supersite study, Atmospheric Chemistry and Physics, 19, 6843–6859, https://doi.org/10.5194/acp-19-6843-2019, 2019.

GBD MAPS Working Group: Burden of Disease Attributable to Major Air Pollution Sources in India: Special Report 21, https://www.healtheffects.org/publication/gbd-air-pollution-india, 2018.

Goetz, J. D., Giordano, M. R., Stockwell, C. E., Christian, T. J., Maharjan, R., Adhikari, S., Bhave, P. V., Praveen, P. S., Panday, A. K., Jayarathne, T., Stone, E. A., Yokelson, R. J., and DeCarlo, P. F.: Speciated online PM$_1$ from South Asian combustion sources – Part 1: Fuel-based emission factors and size distributions, Atmospheric Chemistry and Physics, 18, 14 653–14 679, https://doi.org/10.5194/acp-18-14653-2018, https://www.atmos-chem-phys.net/18/14653/2018/, 2018.

Guo, H., Kota, S. H., Chen, K., Sahu, S. K., Hu, J., Ying, Q., Wang, Y., and Zhang, H.: Source contributions and potential reductions to health effects of particulate matter in India, Atmospheric Chemistry and Physics, 18, 15 219–15 229, https://doi.org/10.5194/acp-18-15219-2018, 2018.

Guttikunda, S.K. and Calori, G. A GIS based emissions inventory at 1 km× 1 km spatial resolution for air pollution analysis in Delhi, India. Atmospheric Environment, 67, 101-111, https://doi.org/10.1016/j.atmosenv.2012.10.040, 2013.

IIT Kanpur: Comprehensive study on air pollution and greenhouse gases (GHGs) in Delhi, A report submitted to the Govt. of NCT Delhi and DPCC Delhi, 2016.

Jaiprakash, Singhai, A., Habib, G., Raman, R. S., and Gupta, T.: Chemical characterization of PM1 aerosol in Delhi and source apportionment using positive matrix factorization, Environmental Science and Pollution Research, 24, 445–462, https://doi.org/10.1007/s11356-016-7708-8, 2017.

Jayarathne, T., Stockwell, C. E., Bhave, P. V., Praveen, P. S., Rathnayake, C. M., Islam, Md. R., Panday, A. K., Adhikari, S., Maharjan, R., Goetz, J. D., DeCarlo, P. F., Saikawa, E., Yokelson, R. J., and Stone, E. A.: Nepal Ambient Monitoring and Source Testing Experiment (NAMaSTE): emissions of particulate matter from wood- and dung-fueled cooking fires, garbage and crop residue burning, brick kilns, and other sources, Atmos. Chem. Phys., 18, 2259–2286, https://doi.org/10.5194/acp-18-2259-2018, 2018.

Ng, N. L., Canagaratna, M. R., Jimenez, J. L., Zhang, Q., Ulbrich, I. M., and Worsnop, D. R.: Real-time methods for estimating organic component mass concentrations from aerosol mass spectrometer data, Environmental Science & Technology, 45, 910–916, https://doi.org/10.1021/es102951k, 2011.

Pant, P., Shukla, A., Kohl, S.D., Chow, J.C., Watson, J.G. and Harrison, R.M. Characterization of ambient PM2. 5 at a pollution hotspot in New Delhi, India and inference of sources. Atmospheric Environment, 109, 178-189, https://doi.org/10.1016/j.atmosenv.2015.02.074, 2015.

Pant, P., Baker, S. J., Goel, R., Guttikunda, S., Goel, A., Shukla, A., and Harrison, R. M.: Analysis of size-segregated winter season aerosol data from New Delhi, India, Atmospheric Pollution Research, 7, 100–109, https://doi.org/10.1016/j.apr.2015.08.001, 2016.

Seinfeld, J. H. and Pandis, S. N.: Atmospheric Chemistry and Physics: From Air Pollution to Climate Change, Third Edition, Wiley, New Jersey, 2016.

Sharma, S. and Mandal, T.: Chemical composition of fine mode particulate matter ($PM_{2.5}$) in an urban area of Delhi, India and its source apportionment, Urban Climate, 21, 106–122, https://doi.org/10.1016/j.uclim.2017.05.009, 2017.

Sharma, S., Mandal, T., Saxena, M., Rashmi, Rohtash, Sharma, A., and Gautam, R.: Source apportionment of PM_{10} by using positive matrix factorization at an urban site of Delhi, India, Urban Climate, 10, 656–670, https://doi.org/10.1016/j.uclim.2013.11.002, 2014.

Srivastava, D., Favez, O., Petit, J.E., Zhang, Y., Sofowotee, U.M., Hopke, P.K., Bonnaire, N., Perraudin, E., Gros, V., Villenave, Albinet, A.: Speciation of organic fractions does matter for aerosol source apportionment. Part 3: Combining off-line and on-line measurements, Science of the Total Environment, 690, 944-955, https://doi.org/10.1016/j.scitotenv.2019.06.378, 2019.

Stockwell, C. E., Christian, T. J., Goetz, J. D., Jayarathne, T., Bhave, P. V., Praveen, P. S., Adhikari, S., Maharjan, R., DeCarlo, P. F., Stone, E. A., Saikawa, E., Blake, D. R., Simpson, I. J., Yokelson, R. J., and Panday, A. K.: Nepal Ambient Monitoring and Source Testing Experiment (NAMaSTE): emissions of trace gases and light-absorbing carbon from wood and dung cooking fires, garbage and crop residue burning, brick kilns, and other sources, Atmos. Chem. Phys., 16, 11043–11081, https://doi.org/10.5194/acp-16-11043-2016, 2016.

Xu, W., Croteau, P., Williams, L., Canagaratna, M., Onasch, T., Cross, E., Zhang, X., Robinson, W., Worsnop, D. and Jayne, J. Laboratory characterization of an aerosol chemical speciation monitor with PM2.5 measurement capability, Aerosol Science and Technology, 51, 69-83, https://doi.org/10.1080/02786826.2016.1241859, 2017.

Sources and atmospheric dynamics of organic aerosol in New Delhi, India: Insights from receptor modeling

Sahil Bhandari[1], Shahzad Gani[2], Kanan Patel[1], Dongyu S. Wang[1], Prashant Soni[3], Zainab Arub[3], Gazala Habib[3], Joshua S. Apte[2], and Lea Hildebrandt Ruiz[1]

[1]McKetta Department of Chemical Engineering, The University of Texas at Austin, Texas, USA
[2]Department of Civil, Architectural and Environmental Engineering, The University of Texas at Austin, Texas, USA
[3]Department of Civil Engineering, Indian Institute of Technology Delhi, New Delhi, India

Correspondence: Lea Hildebrandt Ruiz (lhr@che.utexas.edu), Joshua S. Apte (jsapte@utexas.edu)

Abstract.

Delhi, India, is the second most populated city in the world and routinely experiences some of the highest particulate matter concentrations of any megacity on the planet, posing acute challenges to public health (World Health Organization, 2018). However, the current understanding of the sources and dynamics of PM pollution in Delhi is limited. Measurements at the Delhi Aerosol Supersite (DAS) provide ~~a~~ long-term chemical characterization of ambient submicron aerosol in Delhi, with near-continuous online measurements of aerosol composition. Here we report on source apportionment based on positive matrix factorization (PMF), conducted on 15 months of highly time-resolved speciated submicron non-refractory PM_1 (~~NRPM~~NR-PM_1) between January 2017 and March 2018. We report on seasonal variability across four seasons of 2017 and interannual variability using data from the two winters and springs of 2017 and 2018. We show that a modified tracer-based organic component analysis provides an opportunity for a real-time source apportionment approach for organics in Delhi. ~~Thermodynamic modeling allows estimation~~ Phase equilibrium modeling of aerosols using the extended aerosol inorganics model (E-AIM) predicts equilibrium gas-phase concentrations and allows evaluation of the importance of ventilation coefficient (VC) and temperature in controlling primary and secondary organic aerosol. We also find that primary aerosol dominates severe air pollution episodes.

1 Introduction

Exposure to fine particulate matter (PM) poses significant health risks, especially in densely populated areas (Pope and Dockery, 2006; Apte et al., 2015). The Indian National Capital Region (Delhi NCR, India) is a rapidly growing urban agglomeration and encompasses the second-most populated city in the world with extremely high winter PM concentrations and frequent severe pollution episodes. According to a recent estimate, ~~it~~ Delhi is the world's most polluted megacity, on track to also become the world's most populated megacity by 2028 (World Health Organization, 2018; United Nations, 2018). However, the current understanding of the sources and dynamics of PM pollution in Delhi is limited (Pant et al., 2016b).

Delhi has a long history of studies focused on the quantity and composition of suspended particulate matter ~~in Delhi~~ (Mitra and Sharma, 2002). Several studies have found extremely high PM_{10} concentrations (particulate matter smaller than 10

μm in diameter, $PM_{10} \sim 250$–800 μg m^{-3}) and detected tracer compounds for vehicular emissions, biomass burning, and plastic burning. Large domestic use of fossil fuels and biofuels was found to correlate with especially high mass and number concentrations of PM observed in the evening and at night. These studies captured various aspects of air quality patterns including diurnal variation, weekday–weekend effect, seasonal variation, interannual variation as well as correlations of total

5   particle number and mass concentrations with gas phase species such as SO_2 and NO_2 (Sharma et al., 2003; Mönkkönen et al., 2004, 2005a, b). Other studies have discussed the speciation of mass in smaller particles (Chowdhury et al., 2007; Srivastava et al., 2008; Tiwari et al., 2009). Recent studies such as Pant et al. (2015) have emphasized $PM_{2.5}$, and consistently report high winter concentrations of particulate chloride and nitrate, and high sulfate concentrations across both winter and summer seasons. They attribute chloride to sources such as coal ~~, biomass burning,~~ combustion and biomass

10   and waste burning ~~due to the presence of molecular markerscorresponding to these sources.~~ using molecular markers. For example, hopanes such as S and R homohopane isomers are tracers for coal combustion, PAHs such as phenanthrene and benzo(a)anthracene are tracers for coal and biomass burning, and sugar anhydrosaccharides such as levoglucosan and mannosan are tracers for wood/biomass combustion (Pant et al., 2015). They also attribute higher winter concentrations to condensation of semivolatile ammonium nitrate and ammonium chloride during low-temperature conditions, weaker wind speeds, and

15   shallow atmospheric boundary layer in the winter season (Pant et al., 2015, 2016a). In recent years, detailed source-specific profiles of combustion and non-combustion sources in the Southeast Asian region have been developed as a part of studies such as the Nepal Ambient Monitoring and Source Testing Experiment (NAMaSTE) campaign; for example, to discern between garbage burning and dung burning, tracers such as 1,3,5-Trimethylbenzene and coprostanol have been identified (IIT Bombay, 2008; Stockwell et al., 2016; Goetz et al., 2018; Jayarathne et al., 2018).

20   A recent review of receptor modeling studies with a focus on Delhi shows that most PM-based source apportionment studies have attributed Delhi's pollution to vehicular traffic, fossil fuel combustion, and road dust (Pant and Harrison, 2012). However, the differences in particle size cutoff in different studies and techniques used made it difficult to compare results (Pant and Harrison, 2012). ~~Previous~~ Most receptor modeling studies have principally relied on a small number of daily or multi-day filter-based samples collected over temporally restricted sampling periods, thereby limiting the possible application of factor analysis tech-

25   niques such as positive matrix factorization (PMF) to quantify source contributions for entire seasons at the site. Further, despite Delhi being a continental site, multiple studies attribute significant portions of finer fractions of PM to a sea-salt origin (Sharma et al., 2014; Sharma and Mandal, 2017). Recent studies have also developed bottom-up emissions inventories for the National Capital Territory (NCT) region encompassing the city of Delhi (Guttikunda and Calori, 2013), and conducted multi-season multiple-site $PM_{2.5}$ source apportionment using bottom-up approaches (IIT Kanpur, 2016; ARAI and TERI, 2018). In

30   these bottom-up studies, as well as similar studies across South Asia, emissions sources such as transport, industry, dust, household solid fuel use, and biomass and waste burning are shown to contribute substantially to $PM_{2.5}$ (Conibear et al., 2018; GBD MAPS Working Group, 2018; Guo et al., 2018; Apte and Pant, 2019). Although these studies accounted for primary organic carbon and secondary inorganic species such as sulfate and nitrate, they often provide limited information regarding secondary organics. Comparatively fewer studies have reported on PM_1 composition. One such study

35   attributes winter (December) and spring (March) chloride peaks to be of non-sea-salt origin (Jaiprakash et al., 2017). They also

focus on PM$_1$ composition and source apportionment in Delhi and use HYSPLIT to point to potential chloride sources north-west of the Indian Institute of Technology (IIT) Delhi, such as industries of salt and metal processing and thermal power plants. As for organics, previous studies are mostly limited to the quantification of organic carbon, elemental carbon, polycyclic aromatic hydrocarbons, and water-soluble organic compounds ~~(Sharma and Mandal, 2017; Singh et al., 2011; Pant et al., 2015)~~ (Singh et al., 2011; Pant et al., 2015; Sharma and Mandal, 2017).

The Delhi Aerosol Supersite (DAS) campaign provides ~~a~~ long-term chemical characterization of ambient submicron aerosol in Delhi, with near-continuous online measurements of aerosol composition. Here we report on source apportionment conducted on 15 months of highly time-resolved speciated non-refractory submicron aerosols (~~NRPM~~NR-PM$_1$), including organics (Org), chloride (Chl), ammonium (NH4), sulfate (SO4), ~~chloride, ammonium, sulfate,~~ and nitrate (NO3). We use mass spectrometer data from an ~~aerosol chemical speciation monitor~~ Aerosol Chemical Speciation Monitor (ACSM) in the PMF receptor model at a time resolution of 5–6 minutes. This work improves upon the low time resolution of source apportionment utilizing time-integrated filter-based measurements previously employed in Delhi. Over the campaign, organics accounted for 53% of the submicron mass, followed by inorganics (36%, of which sulfate, nitrate, ammonium, and chloride contributed 13%, 8%, 9%, and 6% respectively) and black carbon (BC) (10%) ~~(Gani et al., 2018)~~(Gani et al., 2019, Fig. 3). Table 1 provides a summary of key DAS bulk measurements.

In this manuscript, we focus on organic aerosol and report seasonal variability for four seasons and interannual variability using data from the two winters and springs of 2017 and 2018.

2   Methods

As a part of the DAS campaign, an Aerosol Chemical Speciation Monitor (ACSM, Aerodyne Research, Billerica, MA) was operated at ~0.1 liters per minute (LPM) at ~1-minute time resolution in a temperature-controlled laboratory on the top floor of a four-story building at IIT Delhi. Additionally, BC, ultraviolet absorbing particulate matter (UVPM) and their difference ΔC were measured using a seven-wavelength aethalometer operated at 1 LPM flowrate and 1-minute time resolution (Magee Scientific Model AE33, Berkeley, CA) (Drinovec et al., 2015). These instruments were on separate sampling lines, both of which had a PM$_{2.5}$ cyclone followed by a water trap and a Nafion membrane diffusion dryer (Magee Scientific sample stream dryer, Berkeley, CA). For the ACSM, the scan speed was set at 200 ms amu^{-1} and pause setting at 125 for a sampling time of 64 s. The ACSM measured mass from mass-to-charge ratio (*m/z*) *m/z* 10 to *m/z* 140. However, all analysis was restricted to *m/z* 120 due to smaller mass and large uncertainties associated with data collected at the higher *m/z*s (Ng et al., 2011b). All essential calibrations such as flow rate calibration, ionizer tuning, quadrupole resolution adjustment, adjustment of multiplier voltage, *m/z* calibration, calibrations for measuring the response factor of nitrate, and relative ionization efficiencies of ammonium and sulfate were performed as recommended. Based on identified issues in the usual jump mode ionization efficiency calibrations, additional single scan mode calibrations for estimating ionization efficiencies were also conducted. For data processing, air-beam corrections and the default relative ion transmission corrections were applied. Full details on the sampling site, instrument setup, operating procedures, and calibrations are described in a separate publication ~~(Gani et al., 2018)~~(Gani et al., 2019).

2.1 Study design

We collected the data used in this manuscript from January 2017 to March 2018. ~~Since the ACSM measures mass spectra at every time point, we obtained a two-dimensional matrix of time points (rows) and mass spectral contributions (columns).~~ We conducted separate PMF analysis for each season, with our data categorized into ~~the six distinct~~ six seasons over these 15 months, as defined by the Indian National Science Academy (2018) (Table 2)~~(Indian National Science Academy, 2018)~~. We used the dataset obtained by averaging every five consecutive measurements for the seasonal PMF runs. Autumn (mid-September to November) is not included in our core analysis due to the unavailability of ACSM data for that period.

PMF2 has been identified as an appropriate receptor modeling technique that can be deployed for quantifying source contributions for air quality management (Belis et al., 2015). Since the ACSM measures mass spectra at every time point, we obtained two-dimensional matrices of time points (rows) and mass spectral contributions (columns). We deployed the PMF2 program to resolve factors from the 2D matrices (Paatero and Tapper, 1994). The Igor PMF Evaluation Tool (PET) was used to conduct PMF2 analysis on this dataset and interpret its results (Ulbrich et al., 2009). Further details on the statistical basis of this method are available elsewhere (Ulbrich et al., 2009; Zhang et al., 2011, and references therein). Briefly, PMF is a bilinear unmixing model that performs deconvolution of mass spectra (MS) into the summation of products of positively constrained mass spectral profiles and their corresponding time series, under the assumption that the mass spectral profiles remain constant in time. The iterative PMF technique does not make any assumptions for source or time profiles. In the process, the model minimizes the weighted least squares error (sum of squares of model error normalized to measurement error), or the summation of squares of scaled residuals of the fit at each *m/z* ~~and each time~~ data point.

We used two alternative approaches for conducting PMF. In one approach, only organic spectral data at a specific set of *m/z*s between *m/z* 12 and *m/z* 120 were selected. This approach is the most commonly used approach, and the reasons for the selection of the specific set of *m/z*s have been described previously (Zhang et al., 2005). In this approach, the concentrations of inorganic species measured by the ACSM were used only as external tracers for interpreting organic PMF factors. However, this technique provides limited information on the ~~extent of the~~ relationship between organic and inorganic species (Sun et al., 2012). We pursued a second approach in which we conducted PMF analysis for organic plus inorganic MS. The inorganic *m/z*s selected represent the underived *m/z*s for each species such that spectral contributions at other *m/z*s can be explained completely by data at these *m/z*s ~~(Jimenez group, 2018; Sun et al., 2012)~~(Sun et al., 2012; Jimenez group, 2018). Thus, we have conducted 12 PMF runs in total (six seasons, organic only and organic-inorganic combined). We refer to the ~~organic-MS-based~~ organic MS–based PMF analysis results as "organic-only PMF" and combined organic-inorganic MS–based PMF analysis results as "combined organic-inorganic PMF" results in the manuscript.

Within the PET tool, we removed spikes (Zhang et al., 2005) from the dataset~~and~~, down-weighted selected weak ~~and~~ (Signal to noise ratio, *SNR*<2) *m/z*s by a factor of 2, and removed bad *m/z*s with ~~a low signal to noise ratio~~*SNR*<0.2. Further, we used the default fragmentation table, and as a result, higher weight was given to mass spectral contribution at *m/z* 44 with which data at *m/z*s 16, 17, and 18 are proportionally related. Accordingly, we down-weighted contributions at these *m/z*s ~~.~~ by a factor of 2. We readjusted the results from PMF analysis to account for underestimation of factor mass based on the selected

*m/z*s only. To account for particle losses, we applied transmission and collection efficiencies after conducting PMF analysis ~~(Gani et al., 2018)~~(Gani et al., 2019).

2.2 Factor selection

We conducted PMF runs for one to six factors and explored the solution space using the tools FPEAK and ~~SEEDs~~SEED. We selected an initial number of ~~p~~ *p* factors based on uncentered correlation coefficients with the factors at the selection ~~p−1~~*p−1*. Other criteria employed to select the number of factors include improvement in the solution's ability to explain residual structure with the addition of a factor and ensuring the 25–75th percentiles of scaled residuals for all *m/z*s are between ±3. Changing ~~SEEDs~~the SEED value initializes the PMF algorithm with different pseudorandom starts. Changing the FPEAK value allows exploring rotations of solutions of a given number of factors. Primarily, we gauged the effect of the changing FPEAK and ~~SEEDs~~ SEED using changes in the fraction of variance explained by different factors, correlations of factors' MS with reference MS, and correlations of factors' time series with the time series of external tracers. Differences between plausible factor solutions in the FPEAK-SEED 2D space are also representative of the uncertainty of the final selected solution for each scenario in Table 2 (Ulbrich et al., 2009). We observed unreasonable MS, weak time series correlations, or rotational ambiguity on changing FPEAK and/or SEED from the default selection of FPEAK=0 and SEED=0. We, therefore, used these default parameter values in our core analysis. Details on factor selection for each PMF run can be found in Supplementary Information (Sect. S1). ~~The~~ We use as reference mass spectra the average mass spectral profiles developed by Ng et al. (2011a) ~~based on previous ACSM and Aerosol Mass Spectrometer (AMS) research are used as reference mass spectra~~and cooking (COA) and coal combustion organic aerosol (CCOA) profiles in the AMS spectral databases (Ulbrich et al., 2017, 2018), and the one with the highest correlation with the mass spectrum of the PMF generated factor (generally, Pearson R ≥0.9) is used for ~~the terminology of the~~ naming the obtained factor (Ng et al., 2011a). This comparison ~~allows~~ enables the separation of factors based on their sources since MS of different factors are characterized by different spectral signature peaks (Zhang et al., 2011). For example, hydrocarbon-like organic aerosol (HOA) is a proxy for fresh traffic and combustion emissions and shows prominent peaks at *m/z*s 55 and 57 and a higher fractional organic signal at *m/z* 43 than *m/z* 44. ~~When available, we used~~ In this study, carbon monoxide (CO) ~~measured~~ was not measured. When available, we used CO measured about 11 km (~7 miles) from our site at a fixed monitoring location RK Puram maintained by the Central Pollution Control Board (CPCB), Government of India as an external traffic and combustion tracer. Further, we also utilized the co-located aethalometer measurements of BC (880 nm) as a traffic tracer. For biomass burning, we used two tracers: (i) ΔC, defined as the difference between UVPM (370 nm) and BC detected by the aethalometer (Wang et al., 2011; Olson et al., 2015; Tian et al., 2019) and (ii) the biomass burning component of black carbon, BC$_{BB}$, estimated using the model of Sandradewi et al. (2008).

3 Results and discussion

In this manuscript, we focus on the components of organic aerosol obtained using organic-only PMF and combined organic-inorganic PMF. We report average seasonal concentrations of organic-only PMF factors in Table 3 and the organic com-

ponent of the organic-inorganic combined PMF factors in Table 4. Our results show that the mass spectral profiles of organic-only PMF factors are consistent with reference profiles. In five of the six seasonal organic-only PMF runs, we obtained only two factors—a mixed hydrocarbon-like organic aerosol (HOA)-biomass burning organic aerosol (BBOA) factor, hereafter referred to as primary organic aerosol (POA), and an ~~oxidized~~ oxygenated organic aerosol (OOA) fac-

5   tor. PMF separated HOA and BBOA factors only in spring 2018, and POA MS for this season was calculated by adding these two factors, weighted by their respective time series contributions. Combined organic-inorganic PMF runs further ~~separate~~ separated the OOA factor but not the POA factor. Advanced factor analysis including ME-2 will be explored in a forthcoming publication to separate the POA factor. Source apportionment conducted in this work was limited to separating primary and secondary OA in all seasons (and further, primary into BBOA and HOA in Spring 2018).

10   Further separation of the factors may be possible with high-resolution data combined with application of factor constraints (Aiken et al., 2009; Elser et al., 2016; Al-Naiema et al., 2018) and source-specific measurements such as metals/metal ions for combustion or biomass burning emissions (Jaiprakash et al., 2017), or α-methylglyceric acid for biogenic secondary OA (Srivastava et al., 2019).

    Figure 1a presents the mean of the seasonal organic-only PMF POA MS averaged over the entire campaign and the reference

15   profile for HOA. The behavior of this POA factor is in line with the reference HOA factor (also, Figs. S1a–f, S2a–g, R>0.9), as suggested by the dominance of hydrocarbon signatures in the spectrum in the series $C_nH_{2n-1}^+$ and $C_nH_{2n+1}^+$ (Ng et al., 2010). At the same time, the fractional contributions of the POA factor at m/zs 29, 60, 73, and 115 are higher compared to the reference HOA factor. These m/zs have higher contributions from biomass burning emissions than traffic-related and other combustion emissions (He et al., 2010; Crippa et al., 2014; Bertrand et al., 2017)—comparison with the reference BBOA profile in Fig.

20   S3 points to the influence of biomass burning on the primary organic aerosol factor. As expected, POA tracers, CO and BC, correlate more strongly with the POA factor than with the OOA factor (Fig. S4a–f).

    Figure ~~1b~~ 1b presents the mean of the seasonal organic-only PMF OOA MS ~~,~~averaged over the entire campaign and the reference profile for OOA. OOA is principally associated with secondary organic aerosol (SOA) (Zhang et al., 2011). Mass spectra of the OOA factors in organic-only PMF correlate strongly with the reference OOA factor (R>0.95) (Figs. S1a–f, S5a–f). Time

25   series of the OOA factors correlate stronger with secondary inorganic species, such as nitrate and sulfate, compared to their correlations with the POA factor time series (~~Figs~~Fig. S4a–f). Figure 2 shows the time series of the organic-only POA and OOA factors for the measurement period. The interplay of sources, meteorology, and ~~reaction chemistry~~ photochemistry results in a sharp variation of PMF factor concentrations across seasons. While POA and OOA concentrations are similar in the colder months, OOA is the more abundant component in the warmer months.

30   The combined organic-inorganic PMF analysis yielded three or four factors. One factor ~~, POA,~~ is predominantly composed of primary organics (accounting for 80–95% of the total factor mass)~~, while an~~—we refer to the organic fraction of that factor as POA. An additional two or three factors emerge as a combination of inorganics and ~~oxidized~~ oxygenated organics—namely, ammonium sulfate (AS) mixed with OOA (ASOOA), ammonium nitrate (AN) mixed with OOA (ANOOA) and ammonium chloride (AC) mixed with ~~OA~~ OOA (ACOOA). The time series correlations of the organic-inorganic combined PMF factors

35   with external tracers are shown in Fig. S6a–f. We refer to the organic mass in these mixed factors as AS-OOA, AN-OOA,

and AC-OOA, respectively. This organic mass accounts for 19–59% (avg. 41%), 21–56% (avg. 45%), and 17–23% (avg. 20%) of the total mass of these mixed factors, respectively. The mass spectrum of the POA from organic-inorganic combined PMF analysis correlates most strongly with the reference HOA and/or BBOA (R>0.9). AS-OOA and AN-OOA correlate most strongly with the reference LVOOA profile (R>0.95, Fig. S7a–f). It is therefore not surprising, as shown in Fig. ~~??~~S8a–c,

5 that the behavior of POA and OOA in combined organic-inorganic PMF is very similar to that of organic-only POA and OOA respectively (POA: Slope~1.08, Intercept~1.6, R^2~0.96, OOA: Slope~0.88, Intercept~-0.4, R^2~0.88). Based on the slope of the time series correlations, the combined organic-inorganic PMF estimates ~~8~~~8% more POA and about 12% less OOA than organic-only PMF, with higher disagreement in warmer months. These differences may be due to a relatively higher m/z 44 fraction in the POA from combined organic-inorganic PMF analysis than the POA from organic-only PMF analysis

10 (Figs. ~~S8–S13a~~S9–S14a). Overall, the MS and time series obtained by combining AS-OOA, AN-OOA, and AC-OOA are very similar to the organic-only PMF OOA MS and time series. The mass spectra and time series of the POA and OOA components obtained using combined organic-inorganic PMF factors and organic-only factors are consistently strongly correlated in each season, as shown in Figs. ~~S8–S13a~~S9–S14a–c.

In Sect.~~3.1~~ 3.1, we discuss the mass spectral profiles and diurnal time series patterns of POA across seasons. In Sect.~~3.2~~ 3.2,

15 we discuss the mass spectral profiles and diurnal time series patterns of ~~oxidized~~ oxygenated organic aerosol from the seasonal organic-only PMF analysis as well as the combined organic-inorganic PMF analysis. In Sect.~~3.3~~ 3.3, we contrast the importance of primary versus secondary organic aerosol. We also compare the full PMF results with the tracer-based organic component results. In Sect.~~3.4~~ 3.4, we investigate interannual variability ~~across~~ between the winters and springs of 2017 and 2018 and shed light on the association of PMF factor concentrations with ventilation-related variables—wind speed, planetary boundary

20 layer height (PBLH), and ventilation coefficient (VC = PBLH × wind speed).

3.1 Primary organic aerosol (POA)

The analysis in this section focuses on PMF factors from the organic-only PMF analysis; as suggested by the mass spectral and time series correlations, the behavior of POA in combined organic-inorganic PMF is very similar to the organic-only POA in each season (~~Fig. ??, Figs. S8–S13a,~~ Figs. S9–S14a–c) and is therefore not discussed here. The factors representing primary

25 organic aerosol have consistently high correlations with hydrocarbon-like organic aerosol and show a varying influence of biomass burning organic aerosol (Fig. S1a–f). To assess the seasonal variability of this biomass burning influence on the mass spectra, Fig. S2a–g compares the mass spectra of the POA factors with reference HOA and BBOA profiles. The mixed POA profiles observed in Delhi have fragments at m/zs 60 and 73, tracers of biomass burning, several times the HOA reference profile average and within 15% of the reference BBOA profile average in winter 2017 and 2018 (Fig. S2a,e). Even in the other three

30 seasons with a mixed POA factor, m/z 60 and 73 have contributions higher than the reference HOA profile average by more than a standard deviation (Fig. S2b–d). This behavior points to the mixing of biomass burning in the POA factor. In spring 2018, the separated HOA and BBOA are in line with their respective reference profiles (Fig. S2f–g). The mixing of HOA and BBOA factors in PMF has been observed in previous studies as well (Aiken et al., 2009; Elser et al., 2016; Al-Naiema et al., 2018). The

deployment of other factorization techniques including the Multilinear Engine (ME-2) algorithm for constraining the presence of POA sources such as cooking and biomass burning is the subject of ongoing work and a forthcoming publication.

The organic-only PMF–based POA diurnal time series patterns exhibit high diurnal, interseasonal, and interannual variability between the winters and springs of 2017 and 2018 and are influenced by episodic pollution events (Table 3, Fig. 3). Peaks in the POA diurnal pattern occur early in the morning and late at night, corresponding to periods of higher traffic. Winter peak POA diurnal concentrations are ~2× diurnal peak in spring, ~3–5× diurnal peak in summer, and ~6–7× diurnal peak in monsoon. Additionally, winter peak POA diurnal concentrations are ~8–10× winter diurnal minima, and this peak-to-minimum ratio dampens in warmer months—decreasing to ~5–6× in summer. We observed larger nighttime (1800–2200 hours) and smaller daytime (0600–0900 hours) POA peaks. As the sun sets, radiative cooling of the ground surface flips the ambient temperature profile in the surface layer, with ambient temperature increasing with altitude. This inversion layer is thermally stable and traps pollutants at nighttime. As the sun rises, radiative heating warms up the ground surface and the ambient temperature profile returns to a decreasing trend with altitude, which is thermally unstable. Thus, the nighttime and daytime periods encounter similar thermal transition phases, albeit in opposite directions (Figs. 3, S15) (Seinfeld and Pandis, 2016). However, the nighttime period is accompanied by minimal photochemical conversion of POA to SOA in the evening, confirmed by the lower OOA, AN-OOA, and AS-OOA concentrations in the evening (Sect. 3.2). These dynamics could explain the larger nighttime and the smaller daytime POA peaks. Despite decreasing PBLH and ventilation coefficient at night (2100–0300 hours) (Fig. S15), POA concentrations are decreasing at night (Fig. 3), likely a consequence of decreasing emissions at nighttime and into the early morning of the next day.

Additionally, the lower temperatures in the mornings and evenings of winter and spring seasons (Figs. 3, S15) also appear to play a role in generating POA peaks at these times. For example, the mean POA concentrations for the coolest 20% of the dataset (mean temperature 12.5°C) were ~53 $\mu g\ m^{-3}$, approximately 3× as high as the POA concentration for all other hours (mean temperature 28°C, mean POA ~19 $\mu g\ m^{-3}$) (Fig. S16c). Finally, the differences in POA diurnal minima across seasons is much smaller than the differences in POA diurnal peaks—the POA diurnal minimum decreases from ~10–12 $\mu g\ m^{-3}$ in winter to ~4 $\mu g\ m^{-3}$ in monsoon, and all seasons seem to approach similar baseline concentrations in the afternoon. According to our analysis using the volatility basis set (VBS) (Donahue et al., 2006), differences in observed concentrations in summer and winter can be explained by thermodynamics (equilibrium partitioning) and meteorology (PBLH, VC) alone, suggesting that sources of POA in Delhi may be similar in all seasons. The detailed methodology and results of the VBS analysis are presented in Supplementary Information (Fig. S17, Sect. S2-VBS Application).

With regard to interannual variability, we observe notable consistency between daytime POA profiles in winter and spring of 2017 and 2018 (0900–1700 hours). However, at nighttime and in early morning, POA concentrations have increased in both seasons in 2018 by as much as ~30 $\mu g\ m^{-3}$. It is well known that the median is robust against extremes and the arithmetic mean (AM) is not. Thus, the relative difference between seasonally averaged mean and median is a qualitative measure of the influence of pollution episodes. Additionally, the magnitude of standard deviation (SD) relative to the arithmetic mean and the

8

magnitude of geometric standard deviation (GSD) relative to the geometric mean (GM) are also evidence of episodic behavior. Indeed, based on these metrics of gauging the influence of episodes, POA is influenced by episodic events in the early morning hours in all seasons (Table 3, Fig. 3). These episodes increase mean POA concentrations over the corresponding median by as much as 20 µg m^{-3}, with the largest episodic events occurring in winters. In relative terms, the largest difference is in summer,

5   when mean POA exceeds the median by as much as 55%. Similarly, though seasonal AM and GM for POA are generally smaller than AM and GM for OOA, their corresponding GSD and SD are larger. This difference is particularly stark in colder months, with POA SD almost twice the OOA SD, despite similar AM. While ubiquitous temporally varying sources such as traffic and cooking are important contributors to the overall POA diurnal patterns, they have stable patterns within seasons associated with working hours and meal consumption. The occurrence of pollution episodes in POA could be a consequence

10   of temperature-related biomass and trash burning (colder periods of day/year), agricultural burning (related to the ~~Rabi and Kharif~~ *Rabi* [winter planting and summer harvesting] and *Kharif* [monsoon planting and autumn harvesting] crop harvesting), fireworks, and bonfires (festivals, e.g., Lohri). POA is the largest contributor to PM during these episodes at our site—e.g., for extreme conditions where NR-PM$_1$ exceeded 200 µg m^{-3}, POA accounted for, on an average, 34% of the NR-PM$_1$ mass (Fig. ~~S17~~S18).

15   It is also important to point out the differences in the HOA and BBOA factors identified in Spring 2018 (Figs.~~4~~ 3, S2f–g). Both HOA and BBOA exhibit episodes in the early morning hours of the day, with higher BBOA concentrations than HOA, and BBOA contribution to total organic mass as high as 38%. In the evening and at night, however, HOA is the larger of the two, contributing as much as 42% to total organic mass. Both components display strong diurnal behavior.

3.2   ~~Oxidized~~ Oxygenated organic aerosol (OOA)

20   **3.2.1   Organic-only PMF mass spectra and diurnal patterns**

Here, we discuss the mass spectral profiles of ~~oxidized~~ oxygenated organic aerosol from the seasonal organic-only PMF analysis as well as the combined organic-inorganic PMF analysis. As shown in Fig. 1b, the observed OOA MS profile averaged across seasons is in line with the reference OOA profile. In every season, mass spectra of the OOA factors in organic-only PMF correlate strongly with the reference OOA factor (R>0.95) (Fig. S1a–f). The mass spectral profiles for each factor are provided

25   in Fig. S5a–f. A large fractional contribution at *m/z* 44 is a signature of the OOA factor. The fragment CO$_2^+$ dominates contributions at *m/z* 44 compared to other fragments and is produced by the thermal decarboxylation and ionization-induced fragmentation of carboxylic acids ~~(Ng et al., 2010)~~(Takegawa et al., 2007). The large fractional contribution at *m/z* 44 is beyond +1 standard deviation from the mean of the reference spectrum for most seasons (Fig. S5a-f). This higher contribution at *m/z* 44 could be a result of rapid photochemical processing of fresh emissions, and/or regional transport of aerosol to the receptor

30   site. The vicinity of the site to local sources suggests that rapid photochemical processing may be more important in causing the high *m/z* 44.

~~Figure 4 shows the diurnal cycle of OOA in different seasons.~~The organic-only PMF–based OOA diurnal time series patterns exhibit high interseasonal, limited diurnal, and minimal interannual variability between the winters and springs of 2017 and

2018 and are not influenced by episodic pollution events (Table 3, Fig. 4). Mean and median OOA concentrations, similar in magnitude at most times of the day in every season, increase during the morning, dip midday, and then increase again at nighttime. At nighttime, OOA concentrations remain stable for several hours into the next day and then increase in the early morning. OOA concentrations increase in the morning hours (~0500–0900 hours) despite increasing atmospheric mixing,

5   pointing to photochemical formation related to primary emissions from traffic and other sources. The midday dip is likely associated with increasing atmospheric mixing and perhaps a reduction in daytime primary emissions. In contrast, nocturnal OOA concentrations are considerably less variable up to about 0400–0500 hours, perhaps representing a lower production rate in the absence of photochemistry. Overall, the timing of local primary emissions, meteorology, and boundary layer dynamics are likely responsible for differing behavior at different times of the day.

10   The diurnal variations of the OOA concentrations are stronger in winter (peak concentration ~1.9–2.3× midday concentration) than in the summer and monsoon (peak concentration ~1.6–1.7× midday concentration). Also, there is a strong seasonality of the factor with diurnal peak OOA concentrations in winter nearly 1.7× those in spring and ~2.9–3.6× those during the summer. Nevertheless, diurnal variations in OOA are weaker than their POA counterparts across seasons. Apart from a weaker diurnal variation, the daytime peaks in OOA are larger than nighttime peaks, and diurnal minima in OOA concentrations vary

15   substantially across seasons. As Fig. 4 shows, absolute OOA concentrations have large differences between winters and other seasons. In winters, the mean and median OOA concentrations never dip below 30 μg m^{-3}, whereas in other seasons they do not increase above 30 μg m^{-3} except for early morning and at night in the spring and monsoon. As for interannual variability, winter and spring 2018 exhibit variations similar to the respective seasons in 2017.

   Except for a brief period in the summer morning, we observe small differences between median and mean OOA concen-

20   trations at different hours of the day across seasons (Fig. 4). Similar conclusions can be drawn from the magnitude of SD compared to AM and GSD compared to GM (Table 3). ~~Pollution episodesoccur in primary emissions~~ ; while seasonal AM and GM for OOA are generally larger than AM and GM for POA, their corresponding SD and GSD are smaller. Concentrations of OOA do not increase substantially during pollution episodes, thereby showing different behavior than POA (Sect.~~3.1); however, as shown here, this behavior does not translate to OOA~~ 3.1).

25 **3.2.2   Combined organic-inorganic PMF mass spectra and diurnal variation**

Incorporating mass spectral data for inorganics in PMF allows further separation of OOA into AS-OOA, AN-OOA, and AC-OOA—a result likely arising from similar volatility of the organic and inorganic components. In this section, we show that chloride, nitrate, and sulfate measured at the site are largely inorganic—as indicated by combined organic-inorganic PMF analysis which groups these species into factors with ammonium. ~~Whereas, the association of organics with inorganics in PMF~~

30 ~~is a result likely arising from similar volatility.~~ In previous work, OOA associated with ammonium nitrate usually has a mass spectrum showing higher fractional contribution at *m/z* 43 (mostly $C_2H_3O^+$), than *m/z* 44 (CO_2^+), where *m/z* 43 is believed to be associated with non-acid oxygenates (Ng et al., 2010). Additionally, these organic aerosols generally have time series reflecting semi-volatile behavior and are labeled semi-volatile ~~oxidized~~ oxygenated organic aerosol (SVOOA) (Zhang et al., 2011). In this study, while AN-OOA exhibits semi-volatile behavior (Fig. 5a), the distribution of AN-OOA profiles and reference SVOOA are

different (R<0.8, all seasons, Fig. S7a–f). Instead, the relative mass spectral contributions are in line with the reference OOA and the LVOOA profiles (R>0.95) (Figs. S7a–f, ~~Figs. S18–S19a~~S19–S20a–f). The strong mass spectral correlation of AN-OOA with reference LVOOA hints at rapid photochemical aging of aerosols in Delhi so that freshly formed oxidized aerosols have a high oxidation state. The mass spectrum of AS-OOA also compares well to the reference OOA and LVOOA profiles (R>0.95, all seasons) (Figs. ~~S5a~~S7a–f, ~~S20-21a~~S21-22a–f). AN-OOA has higher mean mass spectral contribution at *m/z* 43 compared to AS-OOA; however, the mass spectral ~~contributions~~ contribution at *m/z* 44 ~~are~~ is higher in AS-OOA. Additionally, at most high *m/z*s between 70–120, AN-OOA displays higher contributions than AS-OOA, which is likely a result of less processing (Fig. ~~S22a~~S23a–b) (Ng et al., 2010). AS-OOA profiles have a higher contribution at other prominent lower *m/z*s, such as 17, 24, 41, and 55, as well.

The combined organic-inorganic PMF–based AN-OOA and AS-OOA show different time series patterns which change both diurnally and seasonally~~. Figure 6a–b show the diurnal variations~~, pointing to the semi-volatile behavior of AN-OOA and suggesting potential influence of aqueous phase chemistry in the formation of AS-OOA ~~factor time series obtained from combined organic-inorganic PMF analysis.~~at high relative humidity (RH) (Fig. 5a–b). Based on the peak-to-minimum ratio in diurnal variations, AN-OOA shows stronger variations than OOA and AS-OOA (Fig.~~6a~~ 5a–b). Like OOA from organic-only PMF analysis, the smaller nighttime increase in AN-OOA compared to the daytime peak is likely due to the minimal photochemical formation at night. Also ~~,~~ like OOA, concentrations of AN-OOA are higher in winter than in other seasons, with concentrations never dipping below 12.5 μg m^{-3} in winters. Among other seasons, AN-OOA concentrations exceed this value only in spring mornings. Within 2017, the diurnal patterns and the absolute AN-OOA concentrations change dramatically. In winters, summer, and monsoon, diurnal peak AN-OOA concentrations are ~2–5× the diurnal minima; in springs, this ratio increases to ~6–8× . In terms of absolute variations in meteorological variables such as temperature, ~~relative humidity (RH)~~RH, wind speed, and VC, spring shows the most variability (Fig. ~~S14~~S15). These variations might be causing the large peak-to-minimum ratio and the sudden drop in AN-OOA concentrations from winter to spring. The two winters and springs show very similar AN-OOA concentration variations. The mean-median difference, GSD versus GM, and SD versus AM point to episodic behavior in all seasons except winters, possibly due to the semi-volatile behavior of AN-OOA leading to its evaporation at higher temperatures each day (Table 4).

On the other hand, AS-OOA exhibits ~~flatter~~ more flat profiles, especially in the warmer months, with no prominent troughs and a single morning crest only in the colder seasons (winters and springs) (Fig. 5b). Concentrations in winters and springs peak diurnally between 0900–1000 hours, at ~2.0–2.5× the diurnal minima in both winters and ~1.5–1.8× in springs. Warmer seasons have similar peak-to-minima ratios of ~1.5–1.7× in summer and ~1.7–2.0× in monsoon but exhibit ~~flatter~~ more flat profiles in terms of absolute AS-OOA concentrations with mean and median always less than 8 μg m^{-3}. Additionally, high RH ~~>60% occurs in winters and springs~~ conditions generally occur during winter, spring, and monsoon (Fig. ~~S14), and 95th percentile episodes for~~ S15). Very humid conditions are associated with especially high AS-OOA ~~occur predominantly at high RH(Fig. S23~~concentrations. For example, for the highest decile of RH (RH ~90-100%), the mean AS-OOA concentration (~6.4 μg m^{-3}) exceeds the mean of the corresponding AS-OOA concentrations for conditions where RH<90% (~4.6 μg m^{-3}) by ~50% (Fig. S24d). Similar behavior has been observed for the ammonium sulfate aerosols previously measured in Delhi and

elsewhere, particularly in the presence of high organic concentrations, and has been attributed to aqueous phase chemistry (Hu et al., 2011; Wang et al., 2016; Jaiprakash et al., 2017; Sarangi et al., 2018; Wang et al., 2018). Nevertheless, such a correlation does not imply causation; meteorological variables are confounded with each other and with other temporal cycles. The flat and lower AS-OOA ~~concentration levels~~ concentrations during the rest of the day are likely an indicator of the contribution of

5 regional sources to AS-OOA. AS-OOA diurnal profiles capture important processes such as nighttime secondary formation that is perhaps related to biomass burning emissions (winter 2017), morning peaks hinting at the possibility of rapid secondary formation from traffic and biomass burning emissions (winters and springs of 2017 and 2018), and prominent nighttime episodes (winter 2018). Interannual behavior of AS-OOA shows a decrease in winter median throughout the day in 2018 compared to 2017 (lower by as much as 9 $\mu g\ m^{-3}$), and an increase in spring 2018 median AS-OOA concentrations compared to the median

10 in spring 2017 (higher by as much as ~4 $\mu g\ m^{-3}$). The ~~mean–median~~ mean-median difference also suggests some midday episodes in spring 2017; these episodes are not observed in spring 2018. Overall, AS-OOA is less volatile than AN-OOA and shows weaker episodic behavior based on AM versus GM, SD versus AM, and GSD versus GM (Table 4).

Broadly speaking, springs have a larger AS-OOA to AN-OOA ratio relative to the winters and summer. This behavior is likely associated with the transitional meteorology of the spring period, where relatively low temperatures and weak atmospheric

15 mixing coincide with higher photochemistry and relative humidity. Also, GM and median AN-OOA levels in Delhi are higher than AS-OOA only in winters, pointing to the strong influence of temperature on PM formation (the evaporation of semi-volatile compounds in warmer periods), and the importance of less photochemistry in winters. To summarize, despite overall consistency across seasons for OOA, its components AN-OOA and AS-OOA show very different behavior ~~,~~ which changes both diurnally and seasonally.

20 Akin to the associations with ammonium nitrate and ammonium sulfate, some organic components also associate with ammonium chloride (Fig. S7a–f). These organics (AC-OOA) account for 17–23% mass of this factor~~(ACOOA)~~. The median fraction of organics associated with this factor does not exceed 4%. ~~Unlike AS-OOA and AN-OOA, the~~ The mass spectra of these organics ~~are not associated with a specific category of reference OA type. Instead, they~~ resemble oxidized biomass burning aerosol (higher fraction of organics at m/z ~~44 than reference BBOA~~ s 60 and 73 than reference SVOOA profile) (Figs.

25 S7a–f, ~~S24a~~S25a–h). These organics may be associated with the AC factor due to their semi-volatile behavior. Indeed, chloride has been used as a tracer for semi-volatile OOA (Zhang et al., 2011). Additionally, chloride has been used as a tracer for biomass burning, specifically agricultural burning, and more recently ~~,~~ has also been detected in plastic burning (Li et al., 2014a, b; Kumar et al., 2015; Fourtziou et al., 2017). However, as Fig. S6a–b and Fig. S6e–f show, for the four seasons (Winters 2017 and 2018, Springs 2017 and 2018), when significant chloride mass is detected in the particulate phase, the time series

30 of the biomass burning tracers, aethalometer-derived biomass burning component of black carbon, BC_{BB}, and the difference between UVPM and BC, ΔC, do not correlate with this AC factor. ~~Additionally, this factor shows strong directionality, with 87% of the 95th percentile episodes occurring when winds are blowing from the North-Northwest~~ Also, the highest 10% of concentrations of this AC factor (>87 $\mu g\ m^{-3}$) are associated with a strong N-NW ~~) direction compared to about 70% for other factors~~ wind component—this directionality behavior is strongest among all PMF components (Fig. S26a–e). Other OOA

35 components also show similar directionality with weaker strength in the N-NW direction (Fig. S26b, d). In contrast to the

OOA components, extreme POA concentrations are associated with a relatively broad range of wind directions (Fig. S26c). This observation suggests that long-range transport from the prevailing N-NW wind direction may be more important for OOA-associated components than for POA. Since Delhi is in an especially ammonia-rich environment (Warner et al., 2017; Van Damme et al., 2018), these observations also suggests that ammonium chloride is forming from the interaction of upwind chloride sources and fertilizer emissions. One logical source of chloride emissions would be the industrial use of hydrochloric acid (Jaiprakash et al., 2017).

Considering that the combined organic-inorganic PMF results cluster nitrate, chloride, and sulfate with ammonium, our findings suggest that nitrates, chlorides, and sulfates measured by the ACSM in New Delhi are dominated by inorganics, particularly at higher concentrations. This finding is consistent with results from analysis based on tracer ratios. The ON_{NO_x} method, developed by Farmer et al. (2010), estimates organic nitrate (ON) contribution in the NO_3 detected by online mass spectrometers such as the AMS based on the ratio of NO_3 fragments at *m/z* 30 to *m/z* 46. The higher the value relative to the pure ammonium nitrate calibration, the greater the importance of organonitrates. The *m/z* 30 to *m/z* 46 ratio increases from winter to monsoon and does not exceed the calibration ratio (3.6) in winters, pointing to a negligible fraction of organonitrates in winters. Similarly, Wang and Hildebrandt Ruiz (2017) use the correlation of chloride mass at *m/z* 36 to organic mass for evaluating the presence of organochlorides. We observe that chloride *m/z* 36 is very weakly correlated to organics, pointing to the dominance of inorganic chlorides. Finally, Hu et al. (2017) suggest use of the SO^+ to SO_3^+ ratio to estimate the presence of organosulfur species. The range of seasonally representative diurnal median across seasons is 2.4–4.1, agreeing very well with the median values obtained with pure ammonium sulfate calibrations (3.0). This result points to the dominance of inorganic sulfate over organosulfates across seasons. Although the diurnal patterns are stable across seasons, there is a slight upward shift in the median ratio from winter 2017 to spring 2018, pointing to a possible change in the importance of organosulfates.

To summarize, our findings indicate that AN-OOA shows stronger diurnal variability than AS-OOA, and the ratio of AS-OOA to AN-OOA is high in spring likely due to transitional meteorology. Compared to other factors, AS-OOA concentrations show a strong association with high RH, possibly a consequence of aqueous phase chemistry. While chloride has been used as a tracer for biomass burning, we do not see any correlation with the aethalometer-derived biomass burning tracers, and suspect chloride to be of industrial origin. Finally, based on PMF results and tracer ratios and correlations for organic nitrates, chlorides, and sulfates, these species are principally inorganic.

3.3 Primary versus secondary organics

In this section, we summarize the contributions of organics as either primary or secondary using the PMF results. We show that (i) primary emissions are more important in high PM pollution periods, (ii) secondary organic aerosols dominate average concentrations year-round, and (iii) a modified tracer-based organic component evaluation could provide real-time source apportionment of POA and SOA for Delhi (Figs. 6a–b, S27–28).

For fractional POA contributions, the nighttime peak between 1800–2200 hours is larger than the daytime peak between 0500–0800 hours, likely due to reduced photochemistry (Fig. 6a). The diurnal minima in the variations occur between 1200–1500 hours in all seasons, likely due to a combination of reduced sources, increased ventilation, and higher temperatures (Fig. 6a). For winter 2017, although the fraction of POA is generally less than 50%, it nears or exceeds the halfway mark during the early morning traffic hours (0600–0800 hours) and for most hours in the evening and at night (1700–0100 hours), with similar behavior persisting across seasons. These time windows also correspond to periods with the highest POA and highest total concentrations, pointing to the importance of local, primary emissions in the high pollution periods, within a day, within each season, and across seasons (Fig. S18). Relative to colder seasons of winter and spring, warmer months exhibit similar midday POA fractions but diverging lower nighttime fractions. The spring 2018 POA fraction varies between 34–75%, higher than the winters of 2017 and 2018 and spring 2017 (20–68%), and summer 2017 and monsoon 2017 (23–53%). Fractional contributions of OOA to total NR-PM$_1$ exhibit very similar timing of crests and troughs across seasons (Fig. 6b). However, OOA fractions for different seasons converge in the middle of the day and diverge in the early morning and at night, with nighttime fractions in colder months generally lower than the warmer months. This result likely reflects the generally greater influence of primary emissions at night and during colder months. The diurnal OOA fractions peak between 1400–1600 hours at ~66–80%. The profiles rapidly descend to diurnal minima between 25–51% between 1900–2000 hours, likely due to lowered photochemistry and enhanced primary source strength. As for interannual variability between the winters of 2017 and 2018, winter 2018 has lower OOA fractions, particularly at nighttime, by as much as 14%. Further, springs of 2017 and 2018 show large differences in the early morning and at night with OOA in 2018 always contributing less (up to 26% less around midnight). This difference could, in part, be due to the separation of a BBOA factor in spring 2018 that allows deconvolution of the biomass burning component. Despite the changes, the diurnal patterns remain consistent interannually.

We have also compared full PMF results for organic mass with a modified tracer-based organic component evaluation (Ng et al., 2011a). The previously deployed tracer approach utilizes linear scaling of mass at specific *m/z*s to estimate the total mass of each of the three factors—HOA, BBOA, and OOA. Since full PMF mostly yields two factors—proxies for primary and secondary aerosols, we compare primary organic aerosols (POA=HOA+BBOA in our analysis) and secondary organic aerosols (OOA) only. However, for our measurements, this results in the total mass estimated using the tracer-based approach substantially different from the actual organic mass (POA: slope~0.29, intercept~5.4, R~0.76; OOA: slope~0.41, intercept~17.3, R~0.30) (Fig. S27). When we enforce a mass closure on the factors, the tracer-based factors are strongly linearly correlated with results from the full PMF with slopes close to 1 (POA: slope~0.91, intercept~−3.7, R~0.96; OOA: slope~1.09, intercept~3.9, R~0.94) (Fig. S28). Given that the tracer-based approach can be conducted almost instantly, this approach has the potential as an effective real-time source apportionment approach to separate primary from secondary organic aerosol in Delhi.

3.4 Factors influencing organic aerosol concentrations and composition

3.4.1 Effect of meteorological variables on interannual variability

In this section, we test the association of the interannual increase in concentrations in the winters and springs of 2018 compared to 2017 with meteorological variables. Apart from source effects, the changes can be a consequence of changing wind direction, wind speed, temperature, RH, and boundary layer height. Here, we compare the seasonally averaged diurnal patterns of these variables (Fig. ~~S27a~~S29a–d). RH averaged over 2017 winter is up to 10% higher compared to winter 2018 (Fig. ~~S27a~~S29a). However, RH ~~primarily affects the ASOOA factor in high pollution episodes~~ is not strongly correlated with changes in pollutant concentrations (Fig. ~~S23~~S24). At the same time, the temperature between the two winters is within 2°C of each other (Fig. ~~S27b~~S29b). In spring, RH is within 6%, and temperature within 4°C at all hours. Diurnal patterns of wind direction are similar in 2017 and 2018, except in the middle of the day when there is a significant shift of about 28° from N-NW to N-NE in winter (Fig. ~~S27c~~S29c). Between springs~~also~~, there is a slight shift of about 14° towards N-NE late in the evening and night between 2000–2400 hours~~and about 29° between 0500–0800 hours~~. Ventilation coefficients are consistent across the two years, except at nighttime—nighttime median VCs are lower by as much as 80% in winter and spring of 2018 (Fig. ~~S27d~~S29d). Thus, a lower VC for hours of the day when HOA and BBOA are most important could be a key reason behind their higher concentrations. The increase could also be due to an enhancement of sources. ~~Specifically, in~~ In winters, it could also be attributed to the extra period sampled—winter 2018 samples between December 21 and January 14, a period missed in winter 2017.

3.4.2 Effect of ventilation-related variables on factor concentrations

The association of ~~ventilation related variables with organic-inorganic combined~~ ventilation-related variables with combined organic-inorganic PMF factors shows that (i) wind speed ~~does not necessarily provide ventilation~~ is not strongly correlated with pollution loading, and (ii) boundary layer dynamics seem to regulate all components, but to different extents ~~. For all factors, pollution increases with wind speed up to 3.75 ms⁻¹~~(Fig. ~~S28a~~(Fig. S30–32a–e). For all PMF factors, concentrations associated with the lower eight deciles of wind speed (up to ~3.5 ms^{-1}) (~80% of the dataset) show either minimal or no decrease (Fig. S30a–e), while total NR-PM$_1$ shows a subtle decreasing trend with higher WS. This observation is important and points to the limited importance of winds ~~bringing an influx of pollutants in Delhi rather than~~ in providing "ventilation". ~~Winds seem to enhance episodes of primary emissions~~At higher speeds, winds seem to decrease concentrations of the primary components—POA and AC—stronger than the oxidized components. ~~This result might be attributable to incoming wind flow bringing in primary emissions from areas upstream of Delhi that are emission hotspots replete with sources, which has been suggested recently (Jaiprakash et al., 2017). The~~ The factors respond contrastingly to the other component important for "ventilation", the planetary boundary layer height (PBLH) ~~, reflects the disparate response of factors~~ (Fig. ~~S29a~~S31a–e). Going from the ~~5th to 95th percentiles, percent of chloride episodes for PBLH <100 m~~increases from 39% to 85%. In comparison, POA episode fractional contribution increases from about 27% to 66%, whereas AN-OOA increases from about 28% to 41%, and AS-OOA increases from about 26% to 45%. However, temperature~~lowest to the highest deciles in PBLH, concentrations of all PMF factors decrease, with especially sharp drops in the first few deciles of PBLH (<100 m), where inversion conditions

exert a strong control on concentrations of all species. The anticorrelations with wind speed and PBLH have been observed previously, albeit for $PM_{2.5}$ and BC concentrations (Guttikunda and Gurjar, 2012; Tiwari et al., 2013). Temperature and ventilation coefficient are correlated (R~0.6), which implies that the association with boundary layer height is likely convoluted with an association with temperature. Finally, ~~the lowest ventilation coefficientup to 500 m²s⁻¹ displays increasing clustering for higher percentiles of episodes as the selection is made from the 5th to the 95th percentile~~ concentrations of PMF factors decrease with increasing ventilation coefficient, with somewhat larger drops in the concentrations of primary components in comparison to secondary components (Fig. ~~S30a~~S32a–e). ~~The increase is from 40% to 88% for AC, about 31% to 70% for POA and about 30% to 50% for AN-OOA and AS-OOA. Clearly, the modulation is stronger for primary components than secondary components.~~

4 Conclusions

This study provides long-term source apportionment results for a receptor site in New Delhi, the most polluted megacity in the world. For the first time, high time resolution data is available for understanding diurnal patterns and seasonal and interannual changes between the winters and springs of 2017 and 2018 of submicron primary and secondary aerosols. Organic-only PMF analysis yields 2–3 factors—POA (HOA+BBOA) and OOA in every season and HOA and BBOA separating as factors only in spring 2018. ~~However, mass spectral contribution at biomass burning tracers and, correlations with reference MS profiles suggest the influence of biomass burning, especially in colder months.~~ Among factors occurring in every season, POA exhibits the strongest diurnal patterns, with the nighttime peak much larger than the daytime peak. The combined organic-inorganic PMF analysis allows separation of ~~oxidized~~ oxygenated organic aerosols into components based on association with ammonium nitrate and ammonium sulfate. The two components display different diurnal patterns, with AN-OOA showing relatively stronger diurnal patterns and AS-OOA displaying ~~flatter~~ more flat profiles with a sharp rise and descent in the middle of the day, likely associated with photochemical formation. AS-OOA shows a sharp increase in concentrations, especially ~~for 95th percentile episodes~~ at high RH, in line with ~~recent observations of~~ formation influenced by aqueous phase chemistry. AN-OOA mass spectral profiles are very similar to reference LVOOA profiles, despite vicinity to local sources, pointing to the rapid processing of aerosols in Delhi. Chloride, nitrate, and sulfate are mostly inorganic. Analysis using the volatility basis set suggests that differences in temperature and, therefore, equilibrium partitioning, can explain differences in observed winter and summer concentrations. While temperature and ventilation coefficient play a crucial role in determining the organic presence in gas or aerosol phase, the N-NW direction is associated with ~~70% of the 95th percentile episodes for all factors except AC-OOA, for which it further increases to 87%. Increasing wind speed up to 3.75 ms⁻¹ is associated with an enhancement of concentrations, likely due to the influx of emissions from upstream~~ a significant fraction of >90th percentile events for all OOA-associated~~–~~components. In contrast to other variables that control atmospheric ventilation (e.g., PBLH), variation of wind speeds had at most a minimal effect on factor concentrations. Observations indicate that regional OA and ammonium chloride contribute substantially to air pollution in Delhi. Further, primary aerosols such as POA and AC increase whereas secondary aerosols such as AN-OOA and AS-OOA stabilize in the high pollution periods. Thus, primary species are more

important contributors to the high pollution episodes in Delhi ~~despite secondary organics dominating~~ and secondary organics dominate year-round fractional contributions to total organics.

The current Indian legislative and legal framework tasks the responsibility of managing air pollution in Delhi to the Environmental Pollution (Prevention & Control) Authority. The Graded Action Response Plan (GRAP) currently in place accounts for a multitude of local and regional sources contributing to air pollution in Delhi (Ministry of Environment, Forest & Climate Change, Government of India, 2018). Because many bottom-up source apportionment efforts for Delhi are based on local (<50–100 km) scale inventories of primary emissions, they may neglect the important contributions of regionally transported primary and secondary aerosol from upwind regions. Here, we demonstrate the importance of secondary aerosol formed via atmospheric processing. Nevertheless, our results are in broad agreement with these inventories: 1) colder seasons are accompanied by higher concentrations and more diverse sources, including higher biomass burning emissions, 2) a significant aerosol mass fraction in Delhi is attributable to non-local sources, and 3) industries are a significant source of fine particulate matter (Guttikunda and Calori, 2013; IIT Kanpur, 2016; ARAI and TERI, 2018). However, the lack of ~~chemically speciated~~ consistent emission inventories limits the feasibility of ~~implementation of such broad programs restricting economic activity~~ action plans like GRAP, given that their implementation restricts economic activity (CEEW, 2019). The results presented here capture the complexity of aerosols in Delhi by speciating them into different chemical categories and identifying associations of those components with each other and meteorological variables and evaluating their behavior at different times of the day and the year. Because the data presented is highly time-resolved, it can provide critical insight into the diverse sources that contribute to pollution loadings, and similar techniques could be used to measure the efficacy of air pollution regulatory actions. Results from this work address several pressing requirements for air quality management in Delhi including a real-time source apportionment approach for organics, evidence ~~of~~ for extremely high chloride concentrations associated with industrial sources, and ~~providing evidence differentiating high pollution episodic events from~~ evidence for primary components dominating high pollution episodes and secondary components dominating seasonal averages. Future work could utilize these speciated measurements to delve into the identification of potential source locations using back-trajectory analysis.

Data availability. Data published in this manuscript's figures and tables are available via the Texas Data Repository. Underlying research data are also available by request to Lea Hildebrandt Ruiz: lhr@che.utexas.edu

Appendix A: Abbreviations

AC: Ammonium Chloride; AC-OOA: ~~Oxidized~~ Oxygenated Organic Aerosol associated with Ammonium Chloride; ACSM: Aerosol Chemical Speciation Monitor; AMS: Aerosol Mass Spectrometer; AN: Ammonium Nitrate; AN-OOA: ~~Oxidized~~ Oxygenated Organic Aerosol associated with Ammonium Nitrate; AS: Ammonium Sulfate; AS-OOA: ~~Oxidized~~ Oxygenated Organic Aerosol associated with Ammonium Sulfate; BBOA: Biomass Burning Organic Aerosol; BC: Black Carbon; CO:

Carbon Monoxide; CPCB: Central Pollution Control Board; DAS: Delhi Aerosol Supersite; GRAP: Graded Action Response Plan; HOA: Hydrocarbon-like Organic Aerosol; HYSPLIT: NOAA Hybrid Single Particle Lagrangian Integrated Trajectory Model; IIT: Indian Institute of Technology; MS: Mass Spectra; NCR: National Capital Region; N-NW: North-Northwest; NRPMN-NE: North-Northeast; NR-PM$_1$: Non-refractory Submicron Particulate Matter; ON: Organic Nitrate; ON$_{NO_x}$: Method

5 to estimate organonitrate fraction using fragment ratio of NO$_3$ 30 to 46; OOA: Oxidized Oxygenated Organic Aerosol; PBLH: Planetary Boundary Layer Height; PET: PMF Evaluation Tool; PM$_1$: Submicron Particulate Matter; PM$_{10}$: Particulate matter smaller than 10 µm in diameter; PMF: Positive Matrix Factorization; POA: Mixed HOA BBOA; RH: Relative Humidity; SOA: Secondary Organic Aerosol; UVPM: Ultra-Violet absorbing Particulate Matter; VBS: Volatility Basis Set; VC: Ventilation Coefficient; WHO: World Health Organization;

References

Aiken, A. C., Salcedo, D., Cubison, M. J., Huffman, J. A., DeCarlo, P. F., Ulbrich, I. M., Docherty, K. S., Sueper, D., Kimmel, J. R., Worsnop, D. R., Trimborn, A., Northway, M., Stone, E. A., Schauer, J. J., Volkamer, R. M., Fortner, E., de Foy, B., Wang, J., Laskin, A., Shutthanandan, V., Zheng, J., Zhang, R., Gaffney, J., Marley, N. A., Paredes-Miranda, G., Arnott, W. P., Molina, L. T., Sosa, G., and Jimenez, J. L.: Mexico City aerosol analysis during MILAGRO using high resolution aerosol mass spectrometry at the urban supersite (T0) — Part 1: Fine particle composition and organic source apportionment, Atmospheric Chemistry and Physics, 9, 6633–6653, https://doi.org/10.5194/acp-9-6633-2009, 2009.

Al-Naiema, I. M., Hettiyadura, A. P. S., Wallace, H. W., Sanchez, N. P., Madler, C. J., Cevik, B. K., Bui, A. A. T., Kettler, J., Griffin, R. J., and Stone, E. A.: Source apportionment of fine particulate matter in Houston, Texas: insights to secondary organic aerosols, Atmospheric Chemistry and Physics, 18, 15 601–15 622, https://doi.org/10.5194/acp-18-15601-2018, 2018.

Apte, J. S. and Pant, P.: Toward cleaner air for a billion Indians, PNAS, 116 (22), 10 614–10 616, https://doi.org/10.1073/pnas.1905458116, 2019.

Apte, J. S., Marshall, J. D., Cohen, A. J., and Brauer, M.: Addressing global mortality from ambient $PM_{2.5}$, Environmental Science & Technology, 49, 8057–8066, https://doi.org/10.1021/acs.est.5b01236, 2015.

ARAI and TERI: Source apportionment of $PM_{2.5}$ and PM_{10} of Delhi NCR for identification of major sources, https://www.teriin.org/sites/default/files/2018-08/AQM-SA_0.pdf, 2018.

Belis, C., Karagulian, F., Amato, F., Almeida, M., Artaxo, P., Beddows, D., Bernardoni, V., Bove, M., Carbone, S., Cesari, D., and Contini, D.: A new methodology to assess the performance and uncertainty of source apportionment models II: The results of two European intercomparison exercises, Atmospheric Environment, 123, 240–250, https://doi.org/10.1016/j.atmosenv.2015.10.068, 2015.

Bertrand, A., Stefenelli, G., Bruns, E. A., Pieber, S. M., Temime-Roussel, B., Slowik, J. G., Prévôt, A. S., Wortham, H., Haddad, I. E., and Marchand, N.: Primary emissions and secondary aerosol production potential from woodstoves for residential heating: Influence of the stove technology and combustion efficiency, Atmospheric Environment, 169, 65–79, https://doi.org/10.1016/j.atmosenv.2017.09.005, 2017.

CEEW: What is Polluting Delhi's Air? Understanding Uncertainties in Emissions Inventory, https://www.ceew.in/publications/what-polluting-delhi%E2%80%99s-air, 2019.

Chowdhury, Z., Zheng, M., Schauer, J. J., Sheesley, R. J., Salmon, L. G., Cass, G. R., and Russell, A. G.: Speciation of ambient fine organic carbon particles and source apportionment of $PM_{2.5}$ in Indian cities, Journal of Geophysical Research: Atmospheres, 112, https://doi.org/10.1029/2007JD008386, 2007.

Conibear, L., Butt, E., Knote, C., Arnold, S. R., and Spracklen, D. V.: Residential energy use emissions dominate health impacts from exposure to ambient particulate matter in India, Nature Communications, 9, https://doi.org/10.1038/s41467-018-02986-7, 2018.

Crippa, M., Canonaco, F., Lanz, V. A., Äijälä, M., Allan, J. D., Carbone, S., Capes, G., Ceburnis, D., Dall'Osto, M., Day, D. A., DeCarlo, P. F., Ehn, M., Eriksson, A., Freney, E., Hildebrandt Ruiz, L., Hillamo, R., Jimenez, J. L., Junninen, H., Kiendler-Scharr, A., Kortelainen, A.-M., Kulmala, M., Laaksonen, A., Mensah, A. A., Mohr, C., Nemitz, E., O'Dowd, C., Ovadnevaite, J., Pandis, S. N., Petäjä, T., Poulain, L., Saarikoski, S., Sellegri, K., Swietlicki, E., Tiitta, P., Worsnop, D. R., Baltensperger, U., and Prévôt, A. S. H.: Organic aerosol components derived from 25 AMS data sets across Europe using a consistent ME-2 based source apportionment approach, Atmospheric Chemistry and Physics, 14, 6159–6176, https://doi.org/10.5194/acp-14-6159-2014, 2014.

Donahue, N. M., Robinson, A. L., Stanier, C. O., and Pandis, S. N.: Coupled partitioning, dilution, and chemical aging of semivolatile organics, Environmental Science & Technology, 40, 2635–2643, https://doi.org/10.1021/es052297c, 2006.

Drinovec, L., Močnik, G., Zotter, P., Prévôt, A. S. H., Ruckstuhl, C., Coz, E., Rupakheti, M., Sciare, J., Müller, T., Wiedensohler, A., and Hansen, A. D. A.: The "dual-spot" aethalometer: An improved measurement of aerosol black carbon with real-time loading compensation, Atmospheric Measurement Techniques, 8, 1965–1979, https://doi.org/10.5194/amt-8-1965-2015, 2015.

Elser, M., Huang, R.-J., Wolf, R., Slowik, J. G., Wang, Q., Canonaco, F., Li, G., Bozzetti, C., Daellenbach, K. R., Huang, Y., Zhang, R., Li, Z., Cao, J., Baltensperger, U., El-Haddad, I., and Prévôt, A. S. H.: New insights into PM$_{2.5}$ chemical composition and sources in two major cities in China during extreme haze events using aerosol mass spectrometry, Atmospheric Chemistry and Physics, 16, 3207–3225, https://doi.org/10.5194/acp-16-3207-2016, 2016.

Farmer, D. K., Matsunaga, A., Docherty, K. S., Surratt, J. D., Seinfeld, J. H., Ziemann, P. J., and Jimenez, J. L.: Response of an aerosol mass spectrometer to organonitrates and organosulfates and implications for atmospheric chemistry, Proceedings of the National Academy of Sciences, 107, 6670–6675, https://doi.org/10.1073/pnas.0912340107, 2010.

Fourtziou, L., Liakakou, E., Stavroulas, I., Theodosi, C., Zarmpas, P., Psiloglou, B., Sciare, J., Maggos, T., Bairachtari, K., Bougiatioti, A., Gerasopoulos, E., Sarda-Estève, R., Bonnaire, N., and Mihalopoulos, N.: Multi-tracer approach to characterize domestic wood burning in Athens (Greece) during wintertime, Atmospheric Environment, 148, 89–101, https://doi.org/10.1016/j.atmosenv.2016.10.011, 2017.

Gani, S., Bhandari, S., Seraj, S., Wang, D. S., Patel, K., Soni, P., Arub, Z., Habib, G., Hildebrandt Ruiz, L., and Apte, J.: Submicron aerosol composition in the world's most polluted megacity: The Delhi Aerosol Supersite campaign, Atmospheric Chemistry and Physics Discussions, https://doi.org/https://doi.org/10.5194/acp-2018-1066, 2018.

Gani, S., Bhandari, S., Seraj, S., Wang, D. S., Patel, K., Soni, P., Arub, Z., Habib, G., Hildebrandt Ruiz, L., and Apte, J.: Submicron aerosol composition in the world's most polluted megacity: The Delhi Aerosol Supersite study, Atmospheric Chemistry and Physics, 19, 6843–6859, https://doi.org/10.5194/acp-19-6843-2019, 2019.

GBD MAPS Working Group: Burden of Disease Attributable to Major Air Pollution Sources in India: Special Report 21, https://www.healtheffects.org/publication/gbd-air-pollution-india, 2018.

Goetz, J. D., Giordano, M. R., Stockwell, C. E., Christian, T. J., Maharjan, R., Adhikari, S., Bhave, P. V., Praveen, P. S., Panday, A. K., Jayarathne, T., Stone, E. A., Yokelson, R. J., and DeCarlo, P. F.: Speciated online PM$_1$ from South Asian combustion sources – Part 1: Fuel-based emission factors and size distributions, Atmospheric Chemistry and Physics, 18, 14 653–14 679, https://doi.org/10.5194/acp-18-14653-2018, 2018.

Guo, H., Kota, S. H., Chen, K., Sahu, S. K., Hu, J., Ying, Q., Wang, Y., and Zhang, H.: Source contributions and potential reductions to health effects of particulate matter in India, Atmospheric Chemistry and Physics, 18, 15 219–15 229, https://doi.org/10.5194/acp-18-15219-2018, 2018.

Guttikunda, S. and Calori, G.: A GIS based emissions inventory at 1 km × 1 km spatial resolution for air pollution analysis in Delhi, India, Atmospheric Environment, 67, 101–111, https://doi.org/10.1016/j.atmosenv.2012.10.040, 2013.

Guttikunda, S. K. and Gurjar, B. R.: Role of meteorology in seasonality of air pollution in megacity Delhi, India, Environmental Monitoring and Assessment, 184, 3199–3211, https://doi.org/10.1007/s10661-011-2182-8, 2012.

He, L.-Y., Lin, Y., Huang, X.-F., Guo, S., Xue, L., Su, Q., Hu, M., Luan, S.-J., and Zhang, Y.-H.: Characterization of high-resolution aerosol mass spectra of primary organic aerosol emissions from Chinese cooking and biomass burning, Atmospheric Chemistry and Physics, 10, 11 535–11 543, https://doi.org/10.5194/acp-10-11535-2010, 2010.

Hu, D., Chen, J., Ye, X., Li, L., and Yang, X.: Hygroscopicity and evaporation of ammonium chloride and ammonium nitrate: Relative humidity and size effects on the growth factor, Atmospheric Environment, 45, 2349–2355, https://doi.org/10.1016/j.atmosenv.2011.02.024, 2011.

Hu, W., Campuzano-Jost, P., Day, D. A., Croteau, P., Canagaratna, M. R., Jayne, J. T., Worsnop, D. R., and Jimenez, J. L.: Evaluation of the new capture vaporizer for aerosol mass spectrometers (AMS) through field studies of inorganic species, Aerosol Science and Technology, 51, 735–754, https://doi.org/10.1080/02786826.2017.1296104, 2017.

IIT Bombay: Development of air pollution source profiles-Stationary sources, https://www.cpcb.nic.in/displaypdf.php?id= U291cmNlLUVtaXNzaW9uLVByb2ZpbGVzLU5WUy1Wb2x1bWUtT25lLnBkZg==, 2008.

IIT Kanpur: Comprehensive study on air pollution and greenhouse gases (GHGs) in Delhi, http://cerca.iitd.ac.in/files/reports/IITK% 20study%202016.pdf, 2016.

Indian National Science Academy: Seasons of Delhi, https://www.insaindia.res.in/climate.php, 2018.

Jaiprakash, Singhai, A., Habib, G., Raman, R. S., and Gupta, T.: Chemical characterization of PM_1 aerosol in Delhi and source apportionment using positive matrix factorization, Environmental Science and Pollution Research, 24, 445–462, https://doi.org/10.1007/s11356-016-7708-8, 2017.

Jayarathne, T., Stockwell, C. E., Bhave, P. V., Praveen, P. S., Rathnayake, C. M., Islam, M. R., Panday, A. K., Adhikari, S., Maharjan, R., Goetz, J. D., DeCarlo, P. F., Saikawa, E., Yokelson, R. J., and Stone, E. A.: Nepal Ambient Monitoring and Source Testing Experiment (NAMaSTE): emissions of particulate matter from wood- and dung-fueled cooking fires, garbage and crop residue burning, brick kilns, and other sources, Atmospheric Chemistry and Physics, 18, 2259–2286, https://doi.org/10.5194/acp-18-2259-2018, 2018.

Jimenez group: PMF-AMS Analysis Guide—Jimenez Group Wiki, http://cires1.colorado.edu/jimenez-group/wiki/index.php/PMF-AMS_ Analysis_Guide, 2018.

Kumar, S., Aggarwal, S. G., Gupta, P. K., and Kawamura, K.: Investigation of the tracers for plastic-enriched waste burning aerosols, Atmospheric Environment, 108, 49–58, https://doi.org/10.1016/j.atmosenv.2015.02.066, 2015.

Li, J., Song, Y., Mao, Y., Mao, Z., Wu, Y., Li, M., Huang, X., He, Q., and Hu, M.: Chemical characteristics and source apportionment of $PM_{2.5}$ during the harvest season in eastern China's agricultural regions, Atmospheric Environment, 92, 442–448, https://doi.org/10.1016/j.atmosenv.2014.04.058, 2014a.

Li, J., Wang, G., Aggarwal, S. G., Huang, Y., Ren, Y., Zhou, B., Singh, K., Gupta, P. K., Cao, J., and Zhang, R.: Comparison of abundances, compositions and sources of elements, inorganic ions and organic compounds in atmospheric aerosols from Xi'an and New Delhi, two megacities in China and India, Science of the Total Environment, 476–477, 485–495, https://doi.org/10.1016/j.scitotenv.2014.01.011, 2014b.

Ministry of Environment, Forest & Climate Change, Government of India: Graded response action plan for Delhi & NCR, http://cpcb.nic.in/ uploads/final_graded_table.pdf, 2018.

Mitra, A. and Sharma, C.: Indian aerosols: Present status, Chemosphere, 49, 1175–1190, https://doi.org/10.1016/S0045-6535(02)00247-3, 2002.

Mönkkönen, P., Uma, R., Srinivasan, D., Koponen, I., Lehtinen, K., Hämeri, K., Suresh, R., Sharma, V., and Kulmala, M.: Relationship and variations of aerosol number and PM_{10} mass concentrations in a highly polluted urban environment—New Delhi, India, Atmospheric Environment, 38, 425–433, https://doi.org/10.1016/j.atmosenv.2003.09.071, 2004.

Mönkkönen, P., Koponen, I. K., Lehtinen, K. E. J., Hämeri, K., Uma, R., and Kulmala, M.: Measurements in a highly polluted Asian mega city: Observations of aerosol number size distribution, modal parameters and nucleation events, Atmospheric Chemistry and Physics, 5, 57–66, https://doi.org/10.5194/acp-5-57-2005, 2005a.

Mönkkönen, P., Pai, P., Maynard, A., E J Lehtinen, K., Hämeri, K., Rechkemmer, P., Ramachandran, G., Prasad, B., and Kulmala, M.: Fine particle number and mass concentration measurements in urban Indian households, Science of the Total Environment, 347, 131–147, https://doi.org/10.1016/j.scitotenv.2004.12.023, 2005b.

Ng, N. L., Canagaratna, M. R., Zhang, Q., Jimenez, J. L., Tian, J., Ulbrich, I. M., Kroll, J. H., Docherty, K. S., Chhabra, P. S., Bahreini, R., Murphy, S. M., Seinfeld, J. H., Hildebrandt, L., Donahue, N. M., DeCarlo, P. F., Lanz, V. A., Prévôt, A. S. H., Dinar, E., Rudich, Y., and Worsnop, D. R.: Organic aerosol components observed in Northern Hemispheric datasets from aerosol mass spectrometry, Atmospheric Chemistry and Physics, 10, 4625–4641, https://doi.org/10.5194/acp-10-4625-2010, 2010.

Ng, N. L., Canagaratna, M. R., Jimenez, J. L., Zhang, Q., Ulbrich, I. M., and Worsnop, D. R.: Real-time methods for estimating organic component mass concentrations from aerosol mass spectrometer data, Environmental Science & Technology, 45, 910–916, https://doi.org/10.1021/es102951k, 2011a.

Ng, N. L., Herndon, S. C., Trimborn, A., Canagaratna, M. R., Croteau, P. L., Onasch, T. B., Sueper, D., Worsnop, D. R., Zhang, Q., Sun, Y. L., and Jayne, J. T.: An Aerosol Chemical Speciation Monitor (ACSM) for routine monitoring of the composition and mass concentrations of ambient aerosol, Aerosol Science and Technology, 45, 780–794, https://doi.org/10.1080/02786826.2011.560211, 2011b.

Olson, M. R., Garcia, M. V., Robinson, M. A., Rooy, P. V., Dietenberger, M. A., Bergin, M., and Schauer, J. J.: Investigation of black and brown carbon multiple-wavelength-dependent light absorption from biomass and fossil fuel combustion source emissions, Journal of Geophysical Research: Atmospheres, 120, 6682–6697, https://doi.org/10.1002/2014JD022970, 2015.

Paatero, P. and Tapper, U.: Positive matrix factorization: A non-negative factor model with optimal utilization of error estimates of data values, Environmetrics, 5, 111–126, https://doi.org/10.1002/env.3170050203, 1994.

Pant, P. and Harrison, R. M.: Critical review of receptor modelling for particulate matter: A case study of India, Atmospheric Environment, 49, 1–12, https://doi.org/10.1016/j.atmosenv.2011.11.060, 2012.

Pant, P., Shukla, A., Kohl, S. D., Chow, J. C., Watson, J. G., and Harrison, R. M.: Characterization of ambient $PM_{2.5}$ at a pollution hotspot in New Delhi, India and inference of sources, Atmospheric Environment, 109, 178–189, https://doi.org/10.1016/j.atmosenv.2015.02.074, 2015.

Pant, P., Baker, S. J., Goel, R., Guttikunda, S., Goel, A., Shukla, A., and Harrison, R. M.: Analysis of size-segregated winter season aerosol data from New Delhi, India, Atmospheric Pollution Research, 7, 100–109, https://doi.org/10.1016/j.apr.2015.08.001, 2016a.

Pant, P., Guttikunda, S. K., and Peltier, R. E.: Exposure to particulate matter in India: A synthesis of findings and future directions, Environmental Research, 147, 480–496, https://doi.org/10.1016/j.envres.2016.03.011, 2016b.

Pope, C. A. and Dockery, D. W.: Health effects of fine particulate air pollution: Lines that connect, Journal of the Air & Waste Management Association, 56, 709–742, https://doi.org/10.1080/10473289.2006.10464485, 2006.

Sandradewi, J., Prévôt, A. S. H., Szidat, S., Perron, N., Alfarra, M. R., Lanz, V. A., Weingartner, E., and Baltensperger, U.: Using aerosol light absorption measurements for the quantitative determination of wood burning and traffic emission contributions to particulate matter, Environmental Science & Technology, 42, 3316–3323, https://doi.org/10.1021/es702253m, 2008.

Sarangi, B., Aggarwal, S. G., Kunwar, B., Kumar, S., Kaur, R., Sinha, D., Tiwari, S., and Kawamura, K.: Nighttime particle growth observed during spring in New Delhi: Evidences for the aqueous phase oxidation of SO_2, Atmospheric Environment, 188, 82–96, https://doi.org/10.1016/j.atmosenv.2018.06.018, 2018.

Seinfeld, J. H. and Pandis, S. N.: Atmospheric Chemistry and Physics: From Air Pollution to Climate Change, Wiley, 3rd edn., 2016.

Sharma, D. N., Sawant, A. A., Uma, R., and Cocker, D. R.: Preliminary chemical characterization of particle-phase organic compounds in New Delhi, India, Atmospheric Environment, 37, 4317–4323, https://doi.org/10.1016/S1352-2310(03)00563-6, 2003.

Sharma, S. and Mandal, T.: Chemical composition of fine mode particulate matter ($PM_{2.5}$) in an urban area of Delhi, India and its source apportionment, Urban Climate, 21, 106–122, https://doi.org/10.1016/j.uclim.2017.05.009, 2017.

Sharma, S., Mandal, T., Saxena, M., Rashmi, Rohtash, Sharma, A., and Gautam, R.: Source apportionment of PM_{10} by using positive matrix factorization at an urban site of Delhi, India, Urban Climate, 10, 656–670, https://doi.org/10.1016/j.uclim.2013.11.002, 2014.

Singh, D., Gadi, R., and Mandal, T. K.: Characterization of particulate-bound polycyclic aromatic hydrocarbons and trace metals composition of urban air in Delhi, India, Atmospheric Environment, 45, 7653–7663, https://doi.org/10.1016/j.atmosenv.2011.02.058, 2011.

Srivastava, A., Gupta, S., and K. Jain, V.: Source apportionment of total suspended particulate matter in coarse and fine size ranges over Delhi, Aerosol and Air Quality Research, 8, 188–200, https://doi.org/10.4209/aaqr.2007.09.0040, 2008.

Srivastava, D., Favez, O., Petit, J., Zhang, Y., Sofowotee, U., Hopke, P., Bonnaire, N., Perraudin, E., Gros, V., and Villenave, Albinet, A.: Speciation of organic fractions does matter for aerosol source apportionment. Part 3: Combining off-line and on-line measurements, Science of the Total Environment, 690, 944–955, https://doi.org/10.1016/j.scitotenv.2019.06.378, 2019.

Stockwell, C. E., Christian, T. J., Goetz, J. D., Jayarathne, T., Bhave, P. V., Praveen, P. S., Adhikari, S., Maharjan, R., DeCarlo, P. F., Stone, E. A., Saikawa, E., Blake, D. R., Simpson, I. J., Yokelson, R. J., and Panday, A. K.: Nepal Ambient Monitoring and Source Testing Experiment (NAMaSTE): emissions of trace gases and light-absorbing carbon from wood and dung cooking fires, garbage and crop residue burning, brick kilns, and other sources, Atmospheric Chemistry and Physics, 16, 11 043–11 081, https://doi.org/10.5194/acp-16-11043-2016, 2016.

Sun, Y. L., Zhang, Q., Schwab, J. J., Yang, T., Ng, N. L., and Demerjian, K. L.: Factor analysis of combined organic and inorganic aerosol mass spectra from high resolution aerosol mass spectrometer measurements, Atmospheric Chemistry and Physics, 12, 8537–8551, https://doi.org/10.5194/acp-12-8537-2012, 2012.

Takegawa, N., Miyakawa, T., Kawamura, K., and Kondo, Y.: Contribution of Selected Dicarboxylic and ω-Oxocarboxylic Acids in Ambient Aerosol to the m/z 44 Signal of an Aerodyne Aerosol Mass Spectrometer, Aerosol Science and Technology, 41, 418–437, https://doi.org/10.1080/02786820701203215, 2007.

Tian, J., Wang, Q., Ni, H., Wang, M., Zhou, Y., Han, Y., Shen, Z., Pongpiachan, S., Zhang, N., Zhao, Z., Zhang, Q., Zhang, Y., Long, X., and Cao, J.: Emission characteristics of primary brown carbon absorption from biomass and coal burning: Development of an optical emission inventory for China, Journal of Geophysical Research: Atmospheres, 124, 1879–1893, https://doi.org/10.1029/2018JD029352, 2019.

Tiwari, S., Srivastava, A. K., Bisht, D. S., Bano, T., Singh, S., Behura, S., Srivastava, M. K., Chate, D. M., and Padmanabhamurty, B.: Black carbon and chemical characteristics of PM_{10} and $PM_{2.5}$ at an urban site of North India, Journal of Atmospheric Chemistry, 62, 193–209, https://doi.org/10.1007/s10874-010-9148-z, 2009.

Tiwari, S., Srivastava, A., Bisht, D., Parmita, P., Srivastava, M. K., and Attri, S.: Diurnal and seasonal variations of black carbon and $PM_{2.5}$ over New Delhi, India: Influence of meteorology, Atmospheric Research, 125–126, 50–62, https://doi.org/10.1016/j.atmosres.2013.01.011, 2013.

Ulbrich, I., Handschy, A., Lechner, M., and Jimenez, J.: AMS Spectral Database, http://cires.colorado.edu/jimenez-group/AMSsd/, 2017.

Ulbrich, I., Handschy, A., Lechner, M., and Jimenez, J.: High-Resolution AMS Spectral Database, http://cires.colorado.edu/jimenez-group/HRAMSsd/, 2018.

Ulbrich, I. M., Canagaratna, M. R., Zhang, Q., Worsnop, D. R., and Jimenez, J. L.: Interpretation of organic components from positive matrix factorization of aerosol mass spectrometric data, Atmospheric Chemistry and Physics, 9, 2891–2918, https://doi.org/10.5194/acp-9-2891-2009, 2009.

United Nations: World urbanization prospects, https://population.un.org/wup/, 2018.

5 Van Damme, M., Clarisse, L., Whitburn, S., Hadji-Lazaro, J., Hurtmans, D., Clerbaux, C., and Coheur, P.-F.: Industrial and agricultural ammonia point sources exposed, Nature, 564, 99–103, https://doi.org/10.1038/s41586-018-0747-1, 2018.

Wang, D. S. and Hildebrandt Ruiz, L.: Secondary organic aerosol from chlorine-initiated oxidation of isoprene, Atmospheric Chemistry and Physics, 17, 13 491–13 508, https://doi.org/10.5194/acp-17-13491-2017, 2017.

Wang, G., Zhang, R., Gomez, M. E., Yang, L., Levy Zamora, M., Hu, M., Lin, Y., Peng, J., Guo, S., Meng, J., Li, J., Cheng, C., Hu, T., Ren,
10 Y., Wang, Y., Gao, J., Cao, J., An, Z., Zhou, W., Li, G., Wang, J., Tian, P., Marrero-Ortiz, W., Secrest, J., Du, Z., Zheng, J., Shang, D., Zeng, L., Shao, M., Wang, W., Huang, Y., Wang, Y., Zhu, Y., Li, Y., Hu, J., Pan, B., Cai, L., Cheng, Y., Ji, Y., Zhang, F., Rosenfeld, D., Liss, P. S., Duce, R. A., Kolb, C. E., and Molina, M. J.: Persistent sulfate formation from London Fog to Chinese haze, Proceedings of the National Academy of Sciences, 113, 13 630–13 635, https://doi.org/10.1073/pnas.1616540113, 2016.

Wang, G., Zhang, F., Peng, J., Duan, L., Ji, Y., Marrero-Ortiz, W., Wang, J., Li, J., Wu, C., Cao, C., Wang, Y., Zheng, J., Secrest, J., Li,
15 Y., Wang, Y., Li, H., Li, N., and Zhang, R.: Particle acidity and sulfate production during severe haze events in China cannot be reliably inferred by assuming a mixture of inorganic salts, Atmospheric Chemistry and Physics, 18, 10 123–10 132, https://doi.org/10.5194/acp-18-10123-2018, 2018.

Wang, Y., Hopke, P. K., Rattigan, O. V., Xia, X., Chalupa, D. C., and Utell, M. J.: Characterization of residential wood combustion particles using the two-wavelength aethalometer, Environmental Science & Technology, 45, 7387–7393, https://doi.org/10.1021/es2013984, 2011.

20 Warner, J. X., Dickerson, R. R., Wei, Z., Strow, L. L., Wang, Y., and Liang, Q.: Increased atmospheric ammonia over the world's major agricultural areas detected from space, Geophysical Research Letters, 44, 2875–2884, https://doi.org/10.1002/2016GL072305, 2017.

World Health Organization: AAP air quality database, http://www.who.int/phe/health_topics/outdoorair/databases/cities/en/, 2018.

Zhang, Q., Alfarra, M. R., Worsnop, D. R., Allan, J. D., Coe, H., Canagaratna, M. R., and Jimenez, J. L.: Deconvolution and quantification of hydrocarbon-like and oxygenated organic aerosols based on aerosol mass spectrometry, Environmental Science & Technology, 39,
25 4938–4952, https://doi.org/10.1021/es048568l, 2005.

Zhang, Q., Jimenez, J. L., Canagaratna, M. R., Ulbrich, I. M., Ng, N. L., Worsnop, D. R., and Sun, Y.: Understanding atmospheric organic aerosols via factor analysis of aerosol mass spectrometry: A review, Analytical and Bioanalytical Chemistry, 401, 3045–3067, https://doi.org/10.1007/s00216-011-5355-y, 2011.

Table 1. Seasonal summary of PM$_1$ species—the arithmetic mean (AM) for hourly mass concentrations (µg m^{-3}). Adapted from ~~Gani et al. (2018)~~Gani et al. (2019).

	Winter	Spring	Summer	Monsoon
Org	112	61	35	23
NH$_4$	20	10	5.2	4.6
Chl	23	9.5	1.5	0.4
NO$_3$	24	9	3.8	3.6
SO$_4$	16	10	10	10
BC	15	11	9	11
NR-PM$_1$	195	100	55	41

Table 2. Periods for seasonal PMF analysis.

Season	Dates
Winter 2017	Dec 1–Feb 14
Spring 2017	Feb 15–Mar 31
Summer 2017	Apr 1–Jun 30
Monsoon 2017	Jul 1–Sep 15
Winter 2018	Dec 1–Feb 14
Spring 2018	Feb 15–Mar 31

Table 3. Organic-only PMF factor concentrations (µg m^{-3}) split into POA and OOA.

	Arithmetic Mean (SD)		Median		Geometric Mean (GSD)	
	POA	OOA	POA	OOA	POA	OOA
Winter 2017	52 (48)	56 (21)	35	56	36 (2.5)	51 (1.5)
Spring 2017	30 (30)	30 (16)	20	27	20 (2.5)	26 (1.8)
Summer 2017	15 (16)	19 (15)	8	16	9 (2.5)	15 (2.1)
Monsoon 2017	9 (8)	15 (9)	6	13	7 (2.3)	12 (1.9)
Winter 2018	61 (56)	56 (24)	41	54	39 (2.7)	51 (1.6)
Spring 2018[a]	20 (19); 21 (18)	24 (12)	12; 23	17 ~~(4, 67)~~	13 (2.6); 15 (2.6)	21 (1.7)

[a]For spring 2018, we were able to separate POA further into HOA and BBOA factors.

Table 4. Organic component of the organic-inorganic combined PMF factor concentrations (µg m^{-3}) split into POA and OOA. ~~For OOA, we~~ We were able to separate OOA into AN-OOA, AS-OOA, and AC-OOA.

	Arithmetic Mean (SD)		Median		Geometric Mean (GSD)	
	POA	OOA	POA	OOA	POA	OOA
Winter 2017	60 (57)	23 (12); 19 (10); 6 (7)	38	22; 18; 4	38 (3.3)	19 (2.5); 15 (2.2); 3 (5.1)
Spring 2017	31(33)	9 (9); 14 (6); 4 (6)	20	6; 13 ; 2	19 (2.9)	5 (3.5); 12 (1.7); 1 (5.6)
Summer 2017[a]	16 (18)	8 (8); 6 (4)	9	5; 5	10 (2.7)	4 (4.1); 5 (2.2)
Monsoon 2017[a]	11 (9)	2 (2); 4 (3)	8	1; 3	8 (2.5)	1 (3.4); 3 (2.0)
Winter 2018	68(62)	22 (12); 15 (11); 12 (13)	42	20; 12; 6	44 (2.7)	19 (1.9); 12 (2.4); 6 (3.4)
Spring 2018	38(36)	7 (7); 16 (7); 5 (8)	24	4; 15; 1	24 (2.9)	4 (3.4); 14 (2.1); 1 (6.9)

[a]For summer and monsoon, OOA was separated only into AN-OOA and AS-OOA as there was no AC-OOA factor.
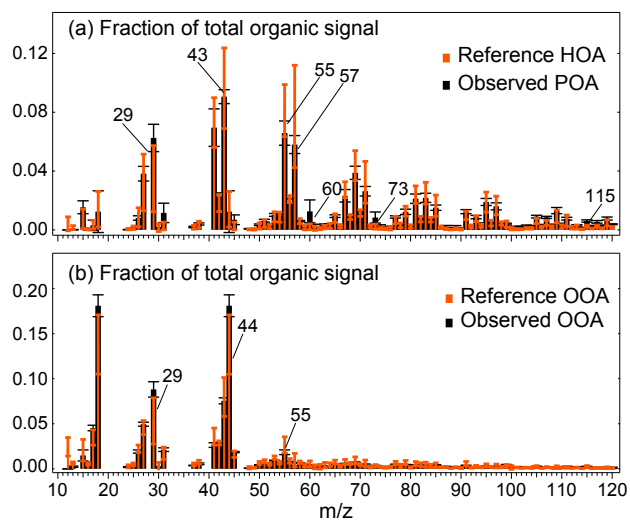
Figure 1. a) The average mass spectrum of organic-only PMF primary organic aerosol (POA) factor shows influence of both hydrocarbon-like organic aerosols (HOA) and biomass burning organic aerosols (BBOA). b) The average mass spectrum of organic-only PMF ~~oxidized~~ oxygenated organic aerosol (OOA) factor ~~, which~~ is similar to the reference OOA factor. The whiskers in the graphs represent ±1 standard deviation from the mean spectra.
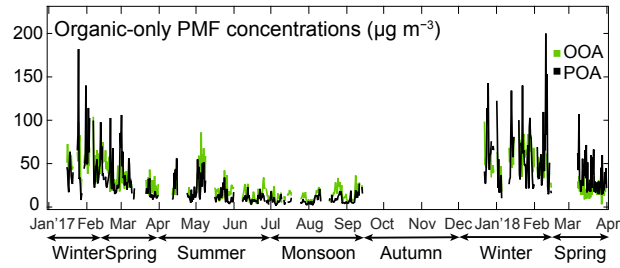
Figure 2. The 12 h averaged concentration time series (TS) of organic-only PMF ~~oxidized~~ oxygenated organic aerosol (OOA) factor and primary organic aerosol (POA) factor ($\mu g\ m^{-3}$). Factor concentrations show strong seasonal ~~and diurnal~~ variations.
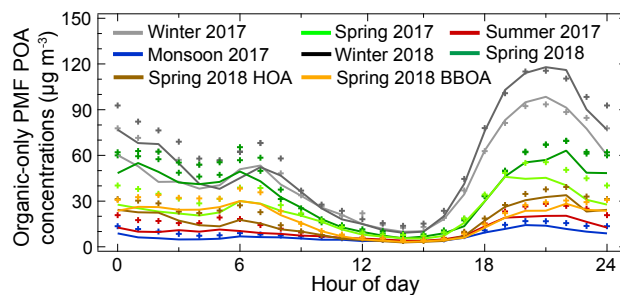
a) Time series correlation of POA and OOA from organic-inorganic PMF and organic-only PMF analysis (g m^{-3}) b) and c) Mass spectral correlations of OOA and POA from organic-inorganic PMF and organic-only PMF analysis. Strong correlations suggest an agreement between the analysis.

Figure 3. Seasonally representative diurnal mean (+) and median concentrations (lines) of POA from organic-only PMF analysis. This figure shows that POA exhibits extreme diurnal variations and displays two peaks corresponding to the early morning and late evening traffic hours.
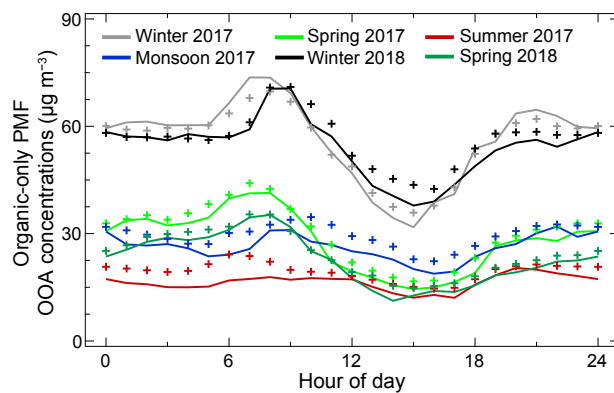
Figure 4. Seasonally representative diurnal mean (+) and median concentrations (lines) of OOA from organic-only PMF analysis. This figure shows the higher concentrations of OOA in winters compared to other months and the relatively stronger diurnal variations in winters and springs compared to other seasons.
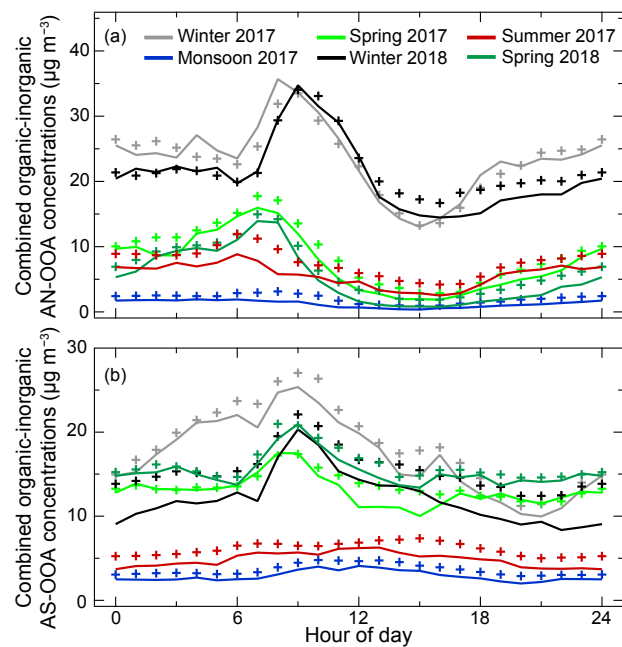
Figure 5. Seasonally representative diurnal mean (+) and median (lines) concentrations of (a) AN-OOA (b) AS-OOA from organic-inorganic combined PMF analysis. Compared to AN-OOA, AS-OOA concentrations remain relatively stable throughout the day, particularly in warmer months.
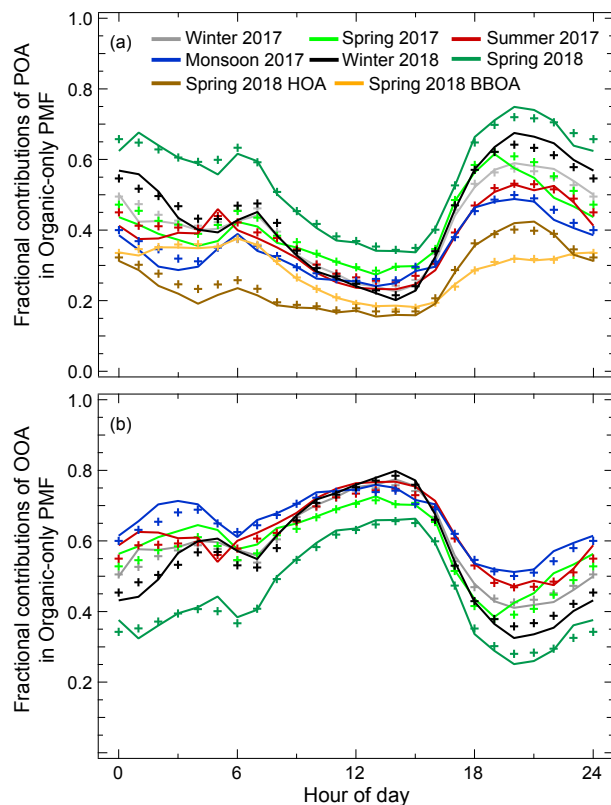
Figure 6. a) Diurnal mean and median composition of POA from organic-only PMF analysis. Spring 2018 has a relatively higher POA fraction, due to the unmixing of a separate BBOA profile. b) Diurnal mean (+) and median (lines) fraction of OOA from organic-only PMF analysis in different seasons. Fractional contributions vary between 32–80%, except spring 2018. This is likely due to the separation of BBOA mixed into the oxidized organics in other seasons. ~~b) Diurnal mean and median composition of POA from organic-only PMF analysis. Spring 2018 has a relatively higher POA fraction, due to the unmixing of a separate BBOA profile.~~

~~This figure shows the comparison of the modified tracer-based OOA and POA concentrations with those obtained from organic-only PMF. The strong linear correlation and slope close to 1 point to the usefulness of the tracer approach for real-time source apportionment.~~